npj | computational materials

Review article

Published in partnership with the Shanghai Institute of Ceramics of the Chinese Academy of Sciences

https://doi.org/10.1038/s41524-024-01412-5

Theoretical approaches for the description of plasmon generated hot carriers phenomena

Mirko Vanzan [1,2] ✉ & Margherita Marsili [3] ✉

Plasmonic-driven photocatalysis is one of the most vibrant and promising field in nanoscience. Out of the various mechanisms known to activate chemical reactions in molecules interacting with optically excited nanostructures, the one involving production and transfer of Hot Carriers (HCs) is among the most relevant. Over the past decade, along with stunning advances on HCs control and manipulation, a variety of theoretical and computational strategies have been developed to model this phenomenon and explore its underlying physics. These techniques have provided comprehensive understandings of HCs life stages and dynamics, and allowed valuable insights on their role in photocatalysis. However, to date it is hard to extricate within the plethora of methods developed and the growing number of applications they found. The purpose of this review is to survey the approaches employed so far to model HCs photophysics, rationalizing and classifying the different studies in terms of modelization, theoretical approaches, and approximations.

The study of light-matter interaction at the nanoscale is driving great research efforts at the corner between physics, chemistry, biology, material science and engineering[1–3]. This because enhancing and manipulating such interaction at the nanometric and sub-nanometric length scales could provide enormous advances on a variety of fields including photonics, catalysis, nanomedicine, and renewable energy[4–6].

Such progresses can be achieved by controlling the excitation of Localized Surface Plasmon Resonance (LSPR), i.e., specific collective oscillatory modes of the electronic cloud, typical of nanoparticles (NPs). By properly tuning structural properties of nanostructures namely their shape and/or composition, it is indeed possible to finely manage the physics of the LSPR and in turn control the wide variety of effects arising from it[7–9].

An important class of technologically relevant phenomena is related to the LSPR decay into Hot Carriers (HCs), out of equilibrium non-thermalized electrons and holes, which have already been exploited in several fields like light harvesting, solar energy and photosensing applications[10–15]. In addition, since the past decade, much effort was spent to understand and optimize the role of HCs dynamics in the field of photocatalysis[16–21]. This opens new perspectives on the technological applications of plasmonic NPs, since they may be used for instance, to effectively exploit solar power as a renewable energy source[22,23] or to produce sustainable fuels starting from simple molecules like water or carbon-dioxide[24–30]. Indeed, the high yield and selectivity commonly found in HCs-mediated reactions[31,32], stimulated the scientific community to understand the mechanism of these processes in details. To date, plasmon enhancement of reaction rates is considered a multifactorial phenomenon possibly triggered by several fundamental processes, such as charge transfer to specific adsorbates' antibonding orbitals, reaction barriers lowering in excited state pathways, resonance of near fields with intramolecular transitions, and local increase of temperature, eventually with some of these processes occurring simultaneously[33–39]. The possible coexistence of all of these effects dramatically increases the complexity of the phenomenon translating into intrinsic difficulties in distinguishing the involved mechanisms. As a consequence, the effects of HCs dynamics can typically be only inferred and not directly observed by experimental techniques[40–42], motivating in turn the large effort spent to investigate the problem using theoretical and computational approaches. Indeed, in the recent years a growing number of theoretical approaches has been applied and/or developed to study plasmonic-generated HCs, causing the proliferation of a rich and original literature. As schematized in Fig. 1, the amount of publications dealing with HCs modeling and simulations dramatically increased over the past decade and is certainly going to grow substantially in the next future[43–45].

The variety of this literature is remarkable: some of the studies simulate directly HCs generation from LSPR dephasing to the chemical reaction ignition, others provide information on HCs dynamics and decays; in some works the system is treated on fully atomistic grounds, in others the plasmonic NPs are treated as a jellium; the electron-electron (e-e) interactions are taken into account at many different levels of accuracy ranging from

[1]Department of Physics, University of Milan, Milano, Italy. [2]Department of Chemical Sciences, University of Padova, Padova, Italy. [3]Department of Physics and Astronomy, University of Bologna, Bologna, Italy. ✉e-mail: mirko.vanzan@unimi.it; margherita.marsili@unibo.it

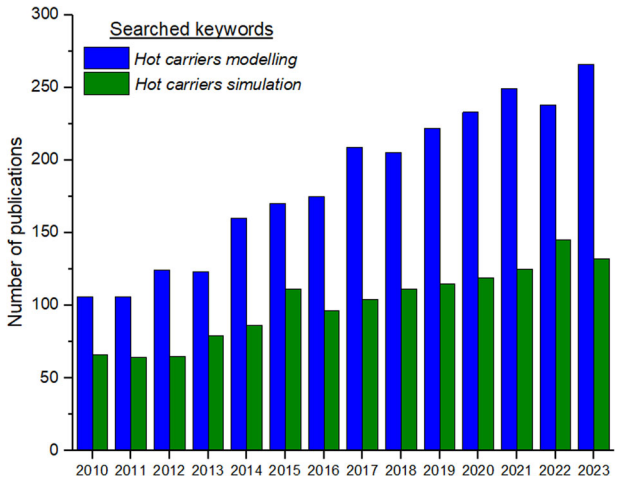

Fig. 1 | Number of publications per year, containing the words "Hot carriers modeling" and "Hot carriers simulation" in their title and/or abstract. Publications include original articles, proceeding papers, reviews, book chapters, early access resources and meeting abstracts. Citation Report graphic is derived from Clarivate Web of Science, Copyright Clarivate 2024. All rights reserved[270,271].

independent particles level to highly correlated quantum chemistry methods; in some cases electron-phonon (e-ph) and electron-holes (e-h) interactions are explicitly considered while in others they are neglected and, finally, the LSPR is either described as an additive effective field acting on the system, or as stemming directly from the electronic system, being one of its possible neutral excitation.

The large amount of methods used to approach this topic is an evidence of the interest it raised over the years, of the challenges it poses and of the different communities that are involved[46]. Rationalizing this huge amount of original theoretical works is the purpose of this review, which is organized as follows. First, we will provide a brief description of the physics behind the HCs phenomena, focusing on their generation, evolution and decays within a metallic NP. We will also describe the various ways in which these carriers can be exploited to catalyze chemical reactions at the NP surface. After that follows the core of this work, where the various strategies developed to investigate HCs phenomena are reviewed and rationalized. A first major distinction here is made between studies employing jellium models and those that adopt an atomistic descriptions of the NP. Within those two frameworks, broad sets of techniques have been developed in order to describe the evolution of the electronic system, going from rate-equation based models[41,47–49], to ab-initio approaches based on Density Functional Theory (DFT) and Many-Body Perturbation Theory (MBPT)[50,51]. A specific section is then devoted to the strategies that allow to increase the size of the simulated systems, focusing in particular on multiscale techniques, where different parts of the system are treated with different level of theoretical sophistication. Finally, perspectives on how the field might develop in the future are provided, taking into account the constraints and limitations that currently affect the available methodologies, and suggesting possible developements while also considering the most recent advances in the field of plasmonics. As Supplementary Information, we provide a brief overview of the main theoretical approaches mentioned in the review, in order to ease readers unfamiliar with these methods to quickly grasp their main features and basic principles. Classical electromagnetic techniques (which are able to describe LSPR features of large metallic NPs, local electric field enhancements and even some features of e-h spatio-temporal dynamics[52]), are already extensively reviewed[53] and thus intentionally left out from the present work when they are not part of a multiscale description of the system.

A challenging problem

A general outline of plasmon generated HCs lifecycle is schematically shown in Fig. 2, panels a–d. Following the optical excitation (Fig. 2a), and disregarding radiative recombination, (which can reasonably be neglected considering small sized NP[54–56]), within the firsts tens of femtoseconds the collective motion of the electronic cloud starts to dephase and decays in e-h pairs (Fig. 2b)[10,57]. Before going on into the description of the fate of these photoinduced electronic excitations, it is worth noting that a unified picture of this preliminary decay is not yet available, as its theoretical description depends on the scheme chosen to model the process and on the assumed corresponding approximations[58]. In particular, there are two major approaches that intimately depend on the description of the LSPR:

(I) the LSPR is considered in its polaritonic nature as a mixed light-electronic mode, either quantizing the corresponding field[59–61] or considering it at the semiclassical level[62], and its decay into e-h pairs is ascribed to the so called Landau damping which, in the quantized case, takes the form of polariton-electron interactions[60]. In this class of approaches the electronic system of the metallic NP is first treated macroscopically, providing a local, space, and frequency-dependent dielectric function $\epsilon(r, \omega)$ which is used to compute the polaritonic local fields by solving the Maxwell's equation with the appropriate boundary conditions given by NP shape and size. Eventually, such fields can be treated as quantum objects, following a quantization procedure[60,63]. Secondly, the electronic system is considered as a quantum system and its interactions with the (classical or quantized) polaritonic field is typically treated at the lowest order of perturbation theory, most of the times using the Fermi's golden rule. In this framework, the effects on e-h pairs generation from the scattering with phonons, defects, and NP surface might also be included[41,58].

(II) The LSPR emerges as one of the possible optical excitation of the electronic system, and is excited by an external electromagnetic field, usually treated classically in the dipole approximation. The decay in e-h pairs is the result of e-e interactions and can be witnessed for example through the analysis of the contributions of single particle transitions at different times[64] or by projecting the system's total density matrix on the basis of the atomic orbitals, to analyze the s, p and d character of the bands HCs populate[65]. In this second class of approaches, the electronic system is treated consistently at a microscopic level throughout the calculations.

The choice of one approach over the other sensibly influences the possible information and interpretation that can be obtained by the computational study, especially the ones focusing on the HCs generation, as we will discuss later. However, in both of these pictures, these preliminary energy and momentum transfers within the electronic system, result in an out-of-equilibrium distribution of the carriers (Fig. 2b) which rapidly relaxes to an equilibrium Fermi-Dirac distribution with an apparent temperature higher than the one of the lattice (see Fig. 2c) through e-e scattering. Without any intervention, carriers thermalize to ambient temperature by e-ph scattering (see Fig. 2d), recovering the original Fermi-Dirac distribution of the NP[66–69]. However, in the presence of appropriate species at the NP interfaces, the energetic carriers could be collected, for instance, into a semiconductor upon overcoming the Schottky barrier[70], or interact with molecular adsorbates triggering chemical reactions.

Several fundamental mechanisms underlie HCs-molecule interactions and their combination/competition drives the molecular evolution toward a specific reaction product[20,71–73]. As schematized in Fig. 2e, the main processes that are possibly involved are:

1. Direct Charge Transfer: the electromagnetic radiation directly excites electrons (or holes) into the target molecule's orbitals leaving a corresponding hole (or electron) in the NP. The presence of this additional charge on the molecule eventually weakens (or strengthens) the interatomic interactions favoring the cleavage (or formation) of certain covalent bonds, in the simplest cases because antibonding (or bonding) orbitals are populated. This process requires the molecular orbitals to be strongly hybridized with the NPs bands and molecular unoccupied levels properly aligned with the HCs distribution;
2. Intramolecular excitation: the optical excitation promotes an intramolecular electronic transition from a molecular binding state to an antibonding orbital. Here, the role of the NP is to provide the near-field enhancement of the radiation impinging the target molecule. The

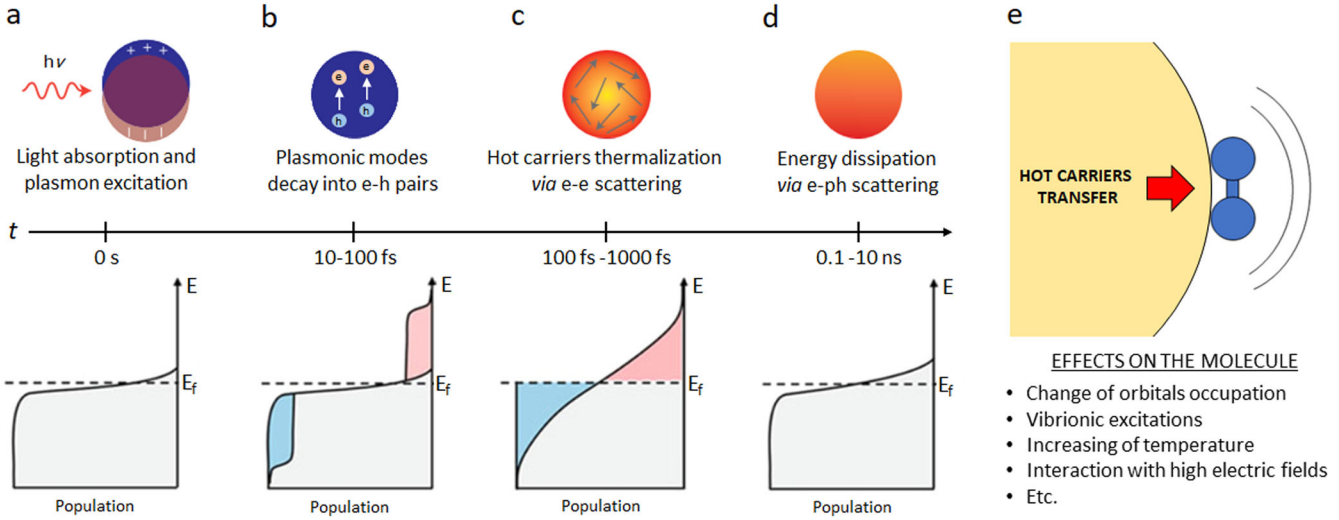

Fig. 2 | HCs life stages and possible effects on molecular adsorbate. a–d Graphical scheme of the different HCs life stages. Upper panels show what happens inside the NP, lower panels display how the occupancy of system's energy levels changes along the process. Central arrow marks the time evolution of the phenomenon. **a** LSPR activation by an external radiation. **b** Plasmon dephasing and subsequent generation of e–h pairs. **c** Intracarriers scattering and electronic cloud thermalization. **d** HCs energy dumping and equilibration to lattice temperature. Adapted with permissions from refs. 11,272 Copyright 2015, 2022 Springer Nature. **e** Scheme and short list of the mechanisms behind HCs catalyzed chemical reactions. Adapted with permissions from ref. 20 Copyright 2023 Springer Nature.

constraint in this case is that the energy of the external field must be resonant with a bright transition leading to the intramolecular excitation;

3. Indirect Charge Transfer: the optical excitation generates an excited e-h pair population within the NP. Subsequently, part of this population moves towards the target molecule. Here what matters is the alignment between the molecular electronic energy levels and the energy of the excited carriers;
4. Transient HCs Spillover: the carriers transiently spill out from the NP and interact with the absorbed species, transferring part of their energy into specific molecular vibrations, which in turn ease the cleavage of chemical bonds. This mechanism, which may be triggered by HCs lying below the molecules antibonding energy level, is not expected to provide much energy to the molecular species, but it could persist as long as the HCs energy is completely dissipated;
5. Increase of Local Temperature: when HCs dissipate their energies by e-ph scattering, the temperature of the system sensibly increases and this induces excitations of molecular vibrational modes which may favor the chemical reaction.

Simulations of HCs generation and evolution allow a fine control over all the factors brought into play and therefore represent a privileged point of view, potentially able to unambiguously unravel the physics behind HCs-related phenomena. Of course such large advantages are balanced by great challenges which are not only ascribed to the modeling of non-equilibrium excited state dynamics of an interacting electronic system (and its eventual coupling to the nuclear degrees of freedom) but also to the presence of different components and different space and time scales. For instance, in the modeling of plasmon-enhanced photocatalysis, the electronic coupling at the NP-adsorbate interface requires an atomistic description of the region, whereas common plasmonic NP size ranges between 10 nm to 100 nm; the LSPR decays within 10 fs, but HCs generation may take 10-100 fs, while the their relaxation occurs in about 100-1000 fs[7,74,75].

In the next sections we will try to summarize and rationalize the efforts that the scientific community has spent to face these challenges in the recent years. In order to ease the discussion on the various methods, in Table 1 we provide a scheme to summarize and quickly compare what will be extensively explored in the following sections.

Jellium models

Within the category 'jellium models', we group all the techniques where the electronic wavefunctions explicitly include only valence electrons, and where core electrons and nuclei are accounted implicitly as an homogeneous background. This kind of modeling has been successfully applied to study HCs generation, relaxation, and transfer as the relatively light amount of computational resources required allows the simulations of large-sized systems (up to tens of nm), properly taking into account the effects coming from NPs geometries, compositions and arrangements. The relative cost-effective use of computational resources makes this technique very flexible and suitable for the investigation of collective plasmonic modes, extrapolation of general trends, and identification of novel effects. However, as they lack of chemical details, these methods do not allow insights related to specific energy level alignments or orbital population. Moreover they can not be used to study dynamical processes involving nuclear dynamics, as in the case of plasmonic-driven chemical reactions. Nevertheless, despite the lack of atomistic resolution, jellium methods provided important insights on the physics underlying HCs dynamics, with the carriers being treated with different levels of theoretical sophistication. In some cases valence electrons are described as independent particles, in others they are subjected to a mean field produced by the other carriers. More refined correlation effects are also included at the DFT or MBPT level. As already mentioned, the plasmonic excitation are either treated as classical (or quantized) field or as one of the possible neutral excitations of the electronic system.

A first basic understanding of HCs generation by LSPR decay using a jellium approach dates back to 2014[62]. Using a semiclassical model the authors considered spherical Ag NPs as free electrons in spherical quantum well, and accounted for the LSPR as a classical field added to the external potential. HCs generation has been evaluated using Fermi golden rule taking into account the optical matrix elements. Although not treating the plasmonic and the single particle excitations at the same level (and thus not taking into account the interplay between the two processes), the work showed how the plasmonic field enhancement is responsible for HCs generation, demonstrating that the rate of this process follows the NP absorption cross-section profile, with a peak at the NP LSPR frequency. As shown in Fig. 3a they also investigated the role that particle size and carrier lifetime have in HCs production and the results qualitatively follow the available experimental data. A similar approach has been employed to investigate HCs production in non-conventional plasmonic materials[76] and

Table 1 | Collection of the methods employed to study HCs photophysics

Modelization	Properties	e-e and e-ph interactions approach	LSPR and e-radiation interactions approach
Jellium NP	HCs generation rates[61,62,76,77,79,138], energy distributions[78,81,82], steady state distributions[83], dynamics[86–88,93], transport across junctions[89–91,263], lifetimes, line widths and decay rates[61,88,95], optical absorption spectra[98,263], field enhancements[98,263]	Free electrons[61,62,76–79,81–83,86,87]; DFT[89]; empirical e-e[83] and e-ph[83,86,87], ab-initio e-e[86–88] scattering rates; HF[93]; GW[88,95]; TDDFT[98,263]	Plasmon: classical[62,76–79] or quantized[61] solution of continuum electromagnetic equations; e-radiation interaction: Fermi golden rule with optical matrix elements[62,76,77], coupling to time-dependent external field within the dipole approximation[98,263]
Atomistic bulk and slab	HCs distributions[60,104,108,109], lifetimes[60,108,109], decay mechanisms[60,108,109], populations dynamics[48,104]; charge and energy transfers[110]; transient absorption spectra[111,112,264,265]; excited state reaction barriers[113,114]	Empirical or fitted e-ph coupling[110,111,264,265]; ab-initio e-e[48,104,109], e-ph[48,60,108,109] scattering rates, electronic heat capacity[111]; DFT[113,114]	Plasmon: quantized solution of continuum electromagnetic equations[48,60,100,108,109]; e-radiation interaction: lowest order interaction vertex[48,60,100,108,109]; ab-initio e-photon-ion collision term[104]
Atomistic NP with frozen nuclei	Absorption spectra[65,98,118–123,126,135,138–149,151–153,178–180,182,185]; line widths[64,119,120,180,182]; single particle transitions[118,121,122,140,141,149,153]; induced charge densities[12,138,139,142–144,152,178,179]; current densities[138,139,152], field enhancements[98,139,180]; time-dependent induced charge densities[64,145–149], transition contributions[64,145,151], populations[65,147,182,185], energy distributions[64,148,185]; HCs generation[145–147,150,184]; charge and energy transfers[146–148,154];	Fd-TDDFT[12,118–123,126,153]; rt-TDDFT[64,98,138–154]; orbital-free TDDFT[178–180]; DFT-parametrized tight-binding with time propagation of the single-particle density matrix[65,182–185,266]	e-radiation interaction: coupling to time-dependent external field within the dipole approximation[28,64,65,118–123,126,138–140,142–151,182,185]
Atomistic NP with nuclear dynamics	Transient absorption spectra[155], time evolution of charge transfers[155], dipole moments[145], HCs energy distributions[145], bond lengths[30,153,161,162,164,171,186], bond energies[267], induced charge densities[161,164], populations[30,69,162,164,167–169,171,186,267,268], orbital energies[69,171,268,269], charge localization[161,167,170,171,186], broadening of plasmon peaks[168]; interfacial charge transfer[165]	TDDFT+Ehrenfest dynamics[30,145,153,155,162,164,191,267]; TDFT +FSSH[69,165,168–171,268,269], P-matrix formalism[167], TD-density functional tight-binding[186]	Excitation modeling: artificial population of unoccupied orbitals[165,167,168], initial configurations from finite temperature adiabatic molecular dynamics[69,169–171,268,269] e-radiation interaction: coupling to time-dependent external field within the dipole approximation[30,145,153,161,162,164,186,267]
All quantum jellium-atomistic multiscale	Time evolution of induced charge densities[24,190], bond lengths[24,190], charge localization[24,190], populations[190], transition contribution coefficients[190]; absorption spectra[24]	TDDFT + Ehrenfest dynamics[24,190]	e-radiation interaction: coupling to a time-dependent external field within the dipole approximation[24,190]
All quantum atomistic multiscale	Induced surface dipoles[102]; plasmonic peaks broadening[102]; ground and excited state reaction pathways[194–199,201]; charge transfers[195]; charge localization along reaction pathway[196];	DFT + HF and CASSCF[102,194]; DFT + CASSCF and NEVPT2[195,198]; DFT + CASPT2[196,197,199–201]	Does not apply to these methodologies
Quantum-classical multiscale	Time evolution of bond lengths[191], energy transfers[223], dipole moments[223]; absorption[191,223,226] and surface-enhanced Raman spectra[213]; extinction coefficients[218]; induced charge densities[223]; decay rates[226], excitation energies[212,214]	TDDFT + discrete interaction models[212,213]; DFT + MM + capacitance polarization model[214]; HF[217,218]; TDDFT + classical electrodynamics[223]; TDDFT + MM + PCM[226]; MBPT + PCM[222]	e-radiation interaction: coupling to a time-dependent external field within the dipole approximation[191,217,223];

Here we classify the main reviewed approaches based on systems modellization, computable quantities, and interactions theoretical backgrounds. Acronyms are defined as follows: Hartree-Fock (HF), Fewest Switches Surface Hopping (FSSH), Complete Active Space Self-Consistent Field (CASSCF), N-Electron Valence state Perturbation Theory up to second order (NEVPT2), Complete Active Space second order Perturbation Theory (CASPT2), classical Molecular Mechanics (MM) and Polarizable Continuum Model (PCM). TDDFT indicates Time-Dependent DFT, prefixes fd- and rt- refer to frequency domain and real time, respectively.

on composite nanosystems[77], suggesting that core@shell NPs composed by an alkaline metal core and a transition metal shell, could present remarkable HCs production rates. Other studies based on similar physical ingredients, i.e., non-interacting electrons confined within potential wells in the presence of an external electromagnetic field plus an additional classical field representing the LSPR (calculated on the basis of Maxwell's equations) treated as a perturbation, showed how the energy distribution of excited carriers strongly correlates to the NP size and, depending on the symmetry of the nanocrystal, also on the polarization of the incident radiation[78,79]. In these studies the enhancement of HCs generation is connected to the non-homogeneity of the plasmonic field, which can be also interpreted as a consequence of the translational symmetry breaking and consequent non-conservation of momentum due to electron-surface scattering[80]. The amplification of carriers generation in a dimer geometry has been also studied, highlighting the important role of hot spots in these kind of nanostructures[81] and to estimate the rate of HCs available for photon upconversion in a metal-semiconductor device, obtaining a 25% yields for small silver nanocubes[82]. Such a theoretical tool has been further refined in 2017 when Besteiro and coworkers computed the rate of hot electrons production depending on the NP size, geometry, and compositions[83]. By including energy-dependent e-e scattering rates, to obtain the steady state distribution of excited electrons, the authors computed the rate of hot electrons production in gold and silver nanosystems with different sizes, arrangements, and morphology. An example of these results is pictured in Fig. 3b where hot electrons production rate in two different Au structures are shown. Such predictions were able to capture the mechanisms underlying LSPR dephasing, namely the Drude-like friction process and further interband carriers excitation, plus the generation of HCs due to surfaces or chemical hot spots. This technique revealed itself as particularly flexible since it could to make predictions on complex NPs shapes (such as nanostars and nanorods), confirming the main role of hot spots in HCs generation[84,85]. Finally a jellium model including a quantized description of the plasmonic field coupled to a non-interacting electrons system has been used to look at the effects that an optically active environment might have into the LSPR decay into e-h pairs[61].

Aiming to investigate HCs relaxation dynamics, a master equation for the time-dependent single-particle population, including the effects of e-e and e-ph scattering, was propagated in time[86,87]. In these works the NPs are

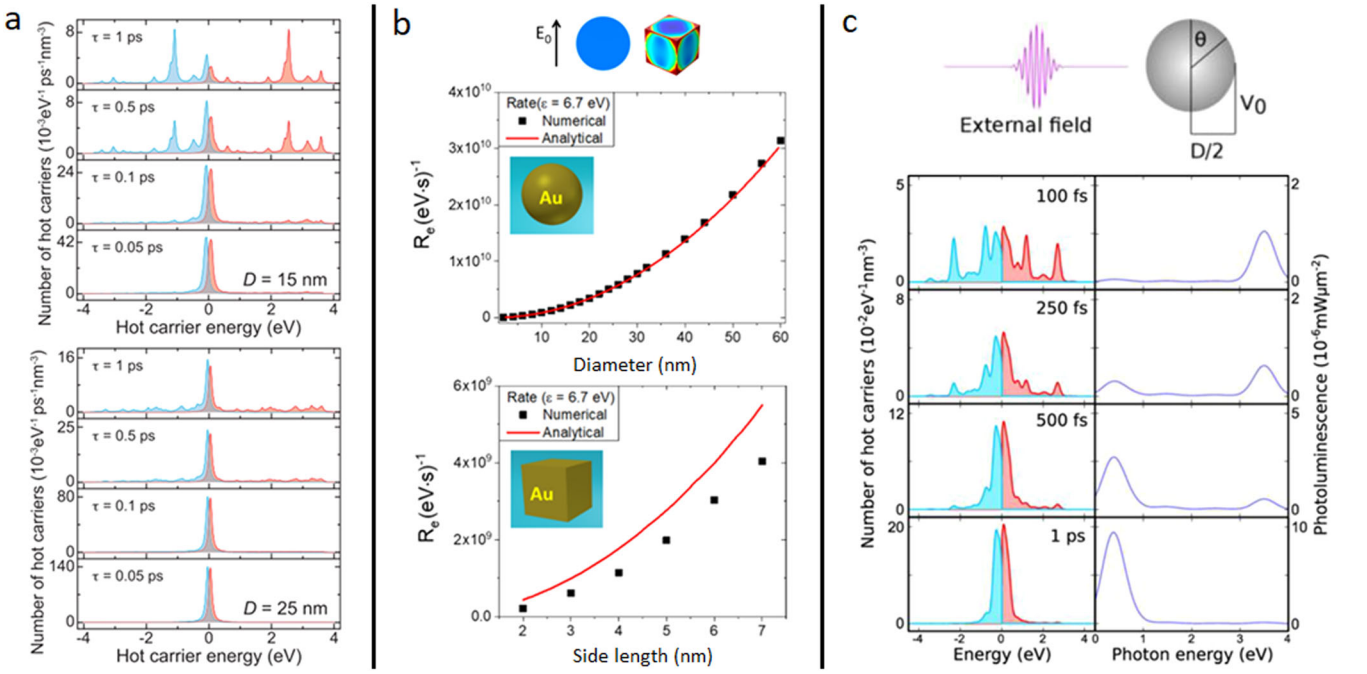

Fig. 3 | Examples of results obtained using jellium models. a HCs distributions upon excitation of Ag nanospheres at plasmon frequency (3.65 eV). Red and blue lines represent the distribution of hot electrons and holes. Top and bottom panels refer to nanospheres with diameter of 15 nm and 25 nm respectively. Distributions obtained using different HCs lifetimes τ. Calculation performed at the semiclassical level, modeling the NP as a jellium. Adapted with permissions from ref. 62 Copyright 2014 American Chemical Society (ACS). **b** Rates of hot electrons generation at 6.7 eV for two different Au nanostructures as a function of their size, modeled through a jellium approach. Systems excited with a radiation matching the LSPR. Graph shows both numerical data and analytical results. Adapted with permissions from ref. 83 Copyright 2017 ACS. **c** Top: scheme of the method adopted to investigate a jellium nanosphere. Bottom: HCs distribution (left) and photoluminecence yield (right) at 100, 250, 500, and 1000 fs upon excitation of LSPR (3.5 eV). In this case Ag nanosphere has a diameter of 6 nm. Red and blue lines represent the distribution of hot electrons and holes respectively. Adapted with permissions from ref. 87 Copyright 2018 ACS.

treated as jellium nanospheres, e-e scattering rates are explicitly computed using a screened Coulomb interaction approach while e-ph scattering rates are empirically parametrized. These studies emphasize the role of e-e scattering and show that, while the time scale of single e-e scattering events is very short (~10 fs), the HCs distribution lifetime is significantly larger (~100–1000 fs) as shown in Fig. 3c. This because hundreds of scattering events per single electron are required for a complete thermalization of the electronic cloud. Similar results have been recently obtained using a model which also account for the HCs generation and further extraction by an attached molecule[88].

Jellium approaches where the electron correlation is treated at the DFT level have been employed to study electron transport through an atomic junction in a plasmonic dimers[89]. Here the authors found a strengthening of the electronic current with the decrease of the NP-NP gap size, and this has been ascribed to the plasmonic local field enhancement which was found being strongly anisotropic and frequency dependent. Similarly in ref. 90 a plasmonic dimer has been modelled as a two levels system, showing that the presence of low energy plasmons can lead to remarkable charge transfers rates if the resonance between the two levels system matches the Fermi energy level of the NPs. Analogous effects on the tunneling currents between NPs and a two levels quantum dot have been also found[91].

Modeling the plasmonic NP as a jellium allowed also to explore the impact a dielectric environment has on HCs generation and thermalization. Using DFT to calculate the effective e-e interaction, it was possible to show how different dielectric environments modifies the NPs density of states and thus influences the HCs production rate. In particular higher generation rates are found when the host materials has large dielectric constants, since it produces larger electron-plasmon couplings[92].

MBPT approaches have been seldomly applied to this kind of systems within the jellium framework. In ref. 93 the authors adopted an equation of motion for the density matrix to study the time-dependent dynamics of photoexcited electrons within a 0.5 nm sphere, treated as a jellium system, including also the Coulomb interaction at the mean-field HF level, yielding resonances shifts and state mixing at the linear response level. The lifetime of single particle excitations for jellium spheres with sizes up to 10 nm have been studied using the GW approximation for the electronic self-energy[94]. The calculated lifetimes are in the femtosecond range and resulted almost independent by the NP size. Their energy dependence however strongly deviates from the bulk one and this is explained in terms of localization of the excited electrons close to the surface, where screening is reduced[95]. More recently, the adoption of MBPT within the GW approximation lead to the estimation of coupling strength of quasiparticles to neutral excitations in a series of sodium NPs[96]. This approach shows how in those systems HCs distributions present discrete peaks, with hot electrons collecting a considerable fraction of the LSPR energy. Moreover, compared to semiclassical models, this approach allowed the estimation of more accurate production rates, especially in smaller NPs.

Ab-initio atomistic approaches, frozen nuclei

While providing important insights on the general mechanism of HCs generation and dynamics, jellium models can not explicitly account for the material dependency of the processes[97]. Indeed the inclusion of the nanosystem's nuclear texture and its consequent well defined band structure, strongly influences optical excitation, carriers' generation rate, transport properties, and fields enhancements[98]. This in turn has remarkable impact in determining absorption spectra, carriers' lifetimes[99], energy and momentum distributions[100], vibronic couplings[101], and the dynamics of carriers population[65]. Moreover, the atomistic structure plays a dominant role in how metal-adsorbate interfaces affect the plasmon damping and therefore deeply affects the photocatalytic properties of the systems[102]. For these reasons, in the past years the computational nanoscience community devoted huge efforts in modeling HCs phenomena using fully atomistic first principles approaches[103].

Such methods indeed explicitly account for the existence of the atomic nuclei, providing a detailed description of the system's electronic band structure. This comes at the cost of a higher consumption of computational resources. Therefore such techniques are typically employed when investigating the opto-electronic properties of small sized structures (composed by hundreds of atoms), and when modeling specific electronic process (such as carriers transfer). However, strong efforts are made in the community to increase the size of the systems that can be studied (see section "Increasing the size of the system"). As summarized in line 2 of Table 1 a first class of studies characterizes the first phases of the LSPR decay through the determination of transport properties such as HCs lifetimes and mean free paths built upon calculations of bulks or slabs-related quantities[48,104,105]. The DFT bulk density of state, for instance, has been used in ref. 104 to build an effective one-band model from which Seibel and coworkers derive the collision integrals for the electron–elctron and absorption terms of the Boltzmann equation for time-dependent electron distribution of noble-metal nanoparticles.

The computational strategy used in these works relies on considering a quantized LSPR field of an infinitely extended interface between a metal, with its own frequency-dependent dielectric function, and a dielectric material, whose electromagnetic response are modelled through a frequency-independent dielectric constant; in the meantime, the coupling of the LSPR with bulk carriers is computed using the lowest order interaction vertex[60,100]. In this framework, the plasmon decay and consequent carriers distributions and lifetimes have been studied for a range of materials using a first principle approach based on DFT coupled with Wannier interpolation methods to calculate the band structure and the entity of e-ph interaction, while the description of e-e contribution to the carriers lifetime relied on the GW approximation[106]. Distinct microscopic decay mechanisms can be evaluated in this way, from direct interband excitations to indirect phonon-assisted and intraband geometry assisted ones[107,108]. As represented in Fig. 4a, these studies show how in the HCs generation phase, the direct excitation mechanism dominates above the interband threshold, while the geometry assisted one, relevant at lower energies, becomes more and more relevant as the size of the system shrinks. The importance of the direct process for Au and Ag is reported also in ref. 60, where similar energy-dependent carriers lifetimes (1 to ~30 fs) and comparable (~10 fs) e-e and e-ph scattering rates and relaxation times were reported[60].

In search for the optimal plasmonic material, the optical properties and carriers lifetimes of bulk transition metal nitrides have been studied using a similar methodology[109]. In this case, the more complex bands structure leads to exotic carrier distributions, covering the entire range from the Fermi level to the photon energy, and interband direct processes dominate HCs generation while the indirect phonon assisted ones are important at lower energies. By combining the aforementioned approach with non-linear Boltzmann equations it was possible to study the excited carriers population dynamics for the interpretation of pump probe experiments in gold NPs[48]. With this setup the authors proved that the optical stimulation generates a non-equilibrium electron distribution, which in the first 100 fs decays and populates levels close to the Fermi energy, thermalizing in ~700 fs. Further thermalization with the lattice happens over several ps.

Concerning ultrafast femtosecond spectroscopies on plasmonic nanostructures, it is worth mentioning in this section the so called Three Temperatures Model (3TM), a semiclassical rate equation approach which typically gets from experiments, but in principle also from ab-initio calculations, part of its microscopic ingredients such as the e-e scattering rates and e-ph coupling coefficients[47]. The rate equations of the 3TM describe the temporal evolution of three energetic variables: the excess energy density of non-thermalized electrons, an electronic term directly related to the optical excitation, and the electronic and lattice temperatures. The dynamics of these three variables are coupled by coefficients that include e-e and e-ph scattering rates and are modulated by temperature dependent electron and lattice heat capacities. This approach has been applied to study the HCs generation yield in metal-oxide nanocomposites decorated by plasmonic Au NP[110], the ultrafast non-radiative relaxation of optically excited free carriers in $CuFeS_2$[111], and more in general the ultrafast dynamics of non-thermal electrons in gold nanostructures[112].

Atomistic slabs models were employed to study how HCs affect reaction energy profiles in plasmonic-driven molecular reactions: combining the DFT - Nudge Elastic Band (NEB) method ΔSCF-DFT (in which the electronic population is constrained in an excited state configuration), it was shown how the presence of extra electrons coming from metallic substrates might promote their evolution towards reduced species[113,114]. Also in these cases the plasmonic NP was modeled as an extended surface; the optical excitation, on the other hand, has been indirectly introduced, mimiking its effect through the presence of an additional electron or an excited e-h pair in the system. When describing the entire NP on atomistic footing, as shown in the third row of Table 1, most of the studies rely on TDDFT, which, within the available approximations of the exchange-correlation kernel, allows the simulations of moderately large and complex structures[115]. Within TDDFT, the LSPR consistently develops as the response of the whole electronic structure to the external field coupled to it through the dipole approximation.

TDDFT equations can be solved either in frequency or time domains. In the frequency domain, a configurational representation in the space of single-particle transitions is used, leading the so called Casida's equations[116]. This approach provides important information on excited states (such as its decomposition in terms of single particle transitions) but is computationally demanding, especially if looking at the high energy part of the spectrum[117,118].

First TDDFT studies of the plasmonic response of metallic nanostructures focused on systems composed of a few tens of atoms. For instance, in 2008 a TDDFT-based determination of the absorption spectra of small Ag nanoclusters (ranging from 20 to 120 atoms) showed how the energy of the main absorption peak, associated to the LSPR, decreases as the size of the nanosystem increases, while the peak width stays approximately constant[119], thus suggesting a common time scale for the dephasing of bright transitions (like the LSPR). Later, the optical responses of Au nanoclusters with sizes up to 172 atoms were analyzed, focusing on the dependence of the LSPR peak position[120]. The results confirmed the picture found on Ag based systems, highlighting at the same time the main role that the system's geometry has in determining the spectral shape. Further insights on Au structures with smaller sizes revealed that the main absorption peaks in the optical spectrum are composed by mixed intraband and interband transitions[121,122]. Frequency-domain TDDFT calculations were succesfully applied also in the case of multi-particles systems[123] nanoalloys[124,125], and demonstrate the existence of long-living triplet excited states in small metallic nanosystems[126]. While novel algorithms based on the complex dynamical polarizability allowed the application of frequency-domain TDDFT also to larger size systems up to ~400 atoms[118,127–133] the standard frequency-domain approach method has been effectively employed also in the study of the optical transitions involved in photocatalysed reactions, such as the reduction of organic molecules over metallic surfaces[134] and the CO_2 methanation over Ag_{25} nanocluster, as show in Fig. 4b[135].

Linear response properties can be addressed within TDDFT also employing real-time propagation (rt-TDDFT). In this case the optical response of the system is obtained by Fourier transforming the real-time evolution of the electronic dipole excited by a delta-like external pulse which equally excites all possible electronic modes. While no energy limitations due to computational burdening is present within rt-TTDFT, part of the information on excited states, such as the single particle transition contributions, is typically lost (although techniques are being developed in order to recover it[136]). Moreover the quality of the simulation and in particular the absorption peaks resolution strongly depends on the choice of calculation parameters such as the trajectory length or the size of the box containing the system (in the real-space framework)[137]. This kind of time propagation is anyway really powerful and largely employed in the study of the optical properties of a variety of systems, including plasmonic structures like nanotube assembly[138] and Na ring dimers[139]. These works showed the effect different incident field polarizations have on various aggregates

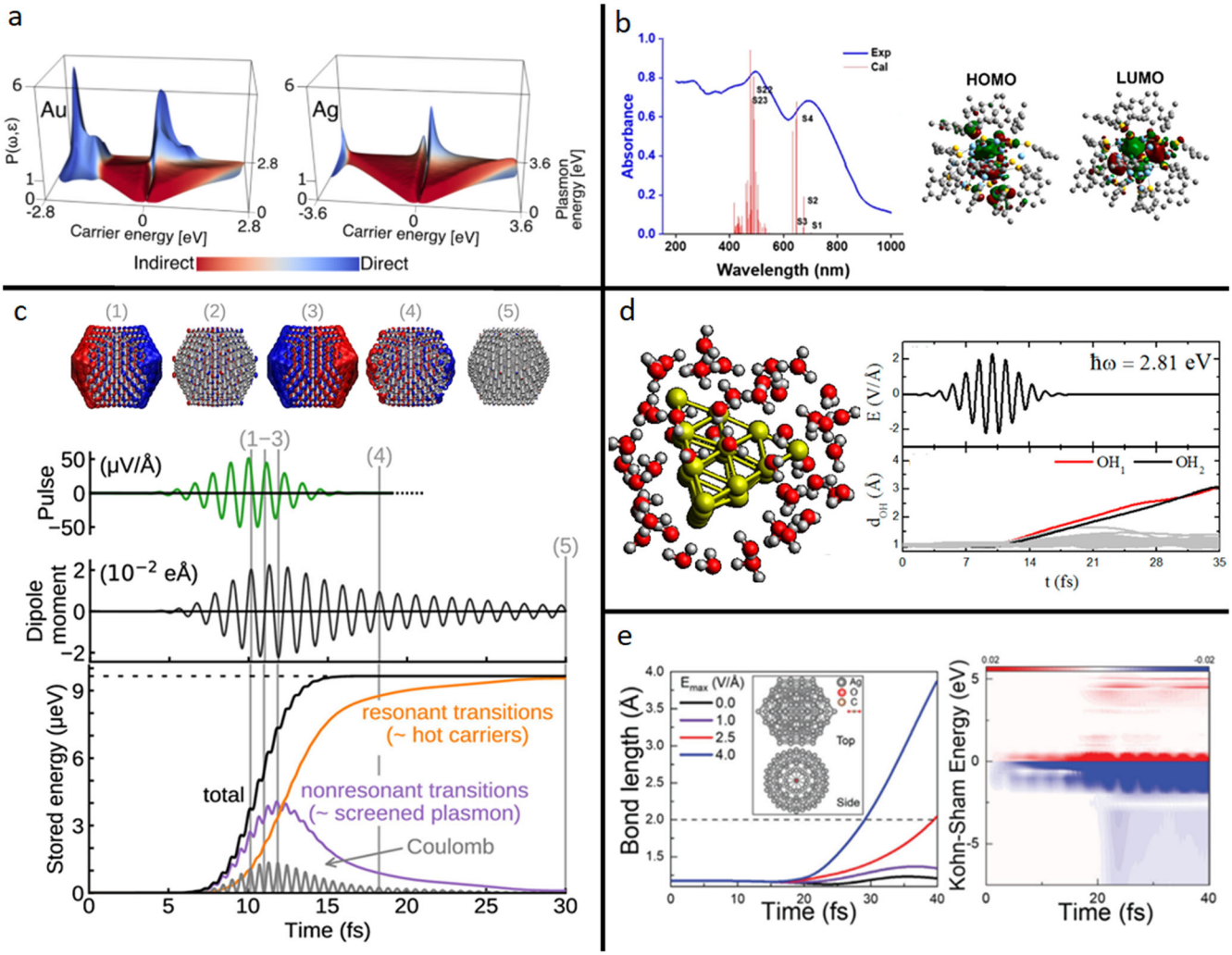

Fig. 4 | Examples of results obtained using ab-initio atomistic models. a HCs energy distribution as a function of plasmon frequency and carrier energy for Au and Ag semi-infinite surfaces. Here the first principle calculations allow to account for the decay of LSPR due to indirect (phonon-assisted, red) and direct (blue) transitions. Adapted with permissions from ref. 108 Copyright 2016 ACS. **b** Experimental absorption spectrum (blue line) and TDDFT calculated excitations (red lines) for the $Ag_{25}(SPhMe_2)_{18}$ cluster. The calculations, based on Casida equation, allow to decompose the excitations into single orbital contributions. Highest Occupied and Lowest Unoccupied Molecular Orbital (HOMO and LUMO) are here depicted as they are involved in several optical excitations. Adapted with permissions from ref. 135 Copyright 2021 ACS. **c**. rt-TDDFT optical response of Ag_{561} NP upon excitation with a laser pulse (green line). Top: (1) to (5) show the oscillations of the electronic density at different time frames; red and blue colors marks electron accumulation and depletion respectively. Bottom: time evolution of NP dipole moment, together with the dynamics of the total energy acquired by the NP, and its decomposition in terms of resonant and non-resonant transitions and Coulomb energy. Adapted from ref. 64 Copyright 2020 Authors, licensed under a Creative Commons Attribution (CC BY) license. **d** Snapshot of Au_{20} nanocluster surrounded by water molecules, together with the time evolution of the laser field and O-H bond lengths (d_{OH}) of the water molecules, calculated coupling rt-TDDFT with Ehrenfest dynamics. Adapted with permissions from ref. 161 Copyright 2018 American Chemical Society. **e** Time evolution of C-O bond length in a Ag_{147}-CO_2 system (shown enclosed) at different electric field intensities (E_{max}) calculated through a Non-Adiabatic Molecular Dynamics (NAMD) approach. On the right side, dynamical changes in the occupation of the Kohn-Sham states obtained upon excitation with a laser pulse where E_{max}= 0.1 V/Å. Adapted from ref. 30 Copyright 2022 Authors, licensed under a CC BY license.

configurations, addressing the origin of the low energy charge-transfer excitation and suggesting a way to tune the optical response based on the relative position of the components. rt-TDDFT allowed also to look at the optical spectra and plasmonic character of excitations in noble and transition metals arrays[140] whereas, in linear metallic chains the dependence of the LSPR with respect to chains lengths and nature has been accurately investigated confirming the presence of non-linear effects connected to the Landau damping of the collective oscillations[141]. As already mentioned, with rt-TDDFT approaches it is possible to investigate systems with larger sizes compared to frequency-domain techniques. For example, it have been possible to explore the LSPR of ichosaedral gold[142] and silver[143] aggregates made of more than 1000, allowing to study the development of the plasmonic modes with increasing cluster sizes and the screening effect caused by the d electrons. The optical spectra of Al and Ag NPs of up to c.a. 560 atoms have been also characterized[144].

Going beyond the determination and characterization of the optical linear response of the system, if the external field is set resonant with the LSPR, rt-TDDFT simulations can be applied to study directly the dynamics of plasmonic HCs witnessing the microscopic mechanisms of generation and injection. For example, in this way, it was possible to study HCs generation in Ag_{55} nanoclusters favored by the presence of single band transitions resonant with the LSPR[145], and HCs injection in a variety of systems: in 2019, a rt-TDDFT study of prototype metal-acceptor interface $Ag_{147}Cd_{33}Se_{33}$ showed the existence of a direct hot electrons transfer between the metallic center and the semiconductor[146], whereas in the case of the Ag_{20} interface with TiO_2, charge separation happened in two steps

consisting in a first fast (~10 fs) electron injection from the cluster to the semiconductor due to the LSPR decay, followed by a second charge sloshing between the two components due to a low frequency charge transfer plasmonic mode[147]. The simulation of CO absorbed on Ag_{147} instead showed how hot electrons stemming from LSPR decay could be actually transferred to the molecular adsorbate and how the transfer probability dependeds on the adsorption site[148]. The important role played by the NP-molecule coupling for HCs generation and injection was also shown in the cases of sodium cluster-hexacene[149] and Ag, Cu, and Au clusters-CO systems[150]. Analysis on the role of the local atomic environment on the HCs generation unveiled how in Ag_{561} the energy of an external pulse is distributed among resonant and non-resonant transitions, with the former responsible for the HCs generation, receiving the largest part of the pulse energy, as shown in Fig. 4c. Moreover with this method it was possible to demonstrate how low-coordinated sites produce larger amounts of hot electrons while hot holes are produced more homogeneously within the NPs, this difference being addressed to the different sp and d character of the bands[64]. In the meantime, a plasmon-mediated non-linear response has been found in the electronic dynamics of an Ag_8 cluster[151]. Linear chains of metallic atoms have been studied to investigate the dynamics and catalytic properties of HCs, demonstrating that molecular bond cleavage can be catalyzed by non-linear effects in tunneling currents[152], plasmonic enhancement of local electric field[153] and by the activation of inner vibrational modes by hot electrons injections[154]. Interestingly, all these studies highlight the paramount importance of the chemical property of molecule over other features such as the NP nature or shape.

Coupling electronic and nuclear motion

Nuclear degrees of freedom and their coupling with the electronic system may influence carriers generation and transfer[60,155]. Indeed, in order to be efficient, charge separation should be faster than energy relaxation through vibrational degrees of freedom and, at the same time, the role of vibrations, associated to local heating, might promote the photocatalytic performance of plasmonic devices[39]. The role of HCs as main actors of photocatalysis is indeed questioned in a number of works that identify pure local thermal enhancement as the source of the high photocatalytic performances of plasmonic systems[36,156–159]. The inclusion of nuclear dynamics in electronic calculations is therefore fundamental to elucidate the competing, or possibly synergic, roles of the various phenomena and is necessary to precisely determine the mechanism of the reactions catalyzed by HCs. Such a huge predictive power however is accompanied by highly cost-intensive simulations. In fact, in addition to the electronic structure and dynamics, these calculations have to consider the ions dynamics and relative phonon structure, and the mutual interactions between nuclei and the excited carriers. Although these aspects can be accounted through various levels of approximation (as we are going to describe in this section), the complexity of the simulations is intrinsically higher compared to frozen-nuclei approaches, making the calculations more computational demanding. These methods are therefore suitable to explore local and specific photochemical processes (such as bond breaking or formation), are not currently usable to model long-lasting phenomena on large-sized systems. Moreover, most of the studies that couple electronic and ionic degrees of freedom employ TDDFT to model the electronic part, using approximated kernels which are not fully adequate for the description of charge transfer phenomena. In this framework, rt-TDDFT coupled to Ehrenfest dynamics[160] has been successfully applied to study the interplay between LSPR decay and vibrational modes in a silver particle composed of 55 atoms[145]. Here e-h pairs generation depends strongly on the availability of single-particle excitations resonant with the plasmon frequency (if available the decay time scale would be in the ~10 fs range, whereas if unavailable a much slower dynamics and Rabi oscillations emerged). In the studied time scale (~100 fs) the effect of e-ph interactions were negligible. Instead, ~ 40 fs seemed enough to activate the cleavage of a O-H bond in H_2O molecule upon photoexcitation of a Au_{20} tetrahedral structure embedded in liquid water, as visible in Fig. 4d[161]. This study showed also the concomitant importance of plasmonic field enhancement and charge transfer from the nanocluster to the antibonding orbitals of the water molecule.

N_2 splitting at the edge of linear silver chains has been studied using the same approach[153,162]. Also in this case, upon photoexcitation of the metallic system, the cleavage of the molecular adsorbate, which can be linked to the direct excitation of charge transfer states involving Ag states and N_2 antibonding orbitals, occurs in tens of fs, well within HCs lifetime (see Fig. 2). This work also elucidated the role played by the external (static or dynamic) electric field in metal-catalyzed H_2 photodissociation[163].

A plasmon enhanced intramolecular charge transfer instead, is responsible for the photodecomposition of NH_3 on Ag clusters simulated within rt-TDDFT and Ehrenfest dynamics[21]. Similar calculations demonstrated that a rapid plasmon-induced water splitting can be obtained by substitution of an Ag atom by a Pb atom in a Ag cluster[164]. Interestingly, without Pb substitution the water molecule would not split. The Pb atom in this case provided both an increase in optical absorption and in the molecule-cluster coupling.

Plasmonic-driven CO_2 photoreduction has been further investigated by means of rt-TDDFT and Ehrenfest dynamics on silver nanostructures finding evidences of a cooperative interplay between indirect and direct HCs transfer, leading to effective photoreduction (see Fig. 4e). Interestingly, these results show that the contributions of the two physical processes can be tuned changing the intensity of the external electromagnetic field[30]. Starting from the population of a plasmonic-like single particle orbital, a combination of rt-TDDFT and NAMD implementing the FSSH technique provided insights on the electron injection dynamics from a photoexcited Au cluster into a TiO_2 surface[165]. The delocalization of the excited state lead to an immediate charge transfer with 50% probability. In the remainig 50% of times the e-h pair is generated within the NP and the electrons are subsequently transferred to the TiO_2 slab within 100 fs while releasing energy to the lattice phonons. A follow up study on similar NP-semiconductor systems reveal that charge transfer can occur according to both the direct and indirect mechanisms described in the section “A challenging problem”, which can coexist and cooperate providing a faster and more effective charge separation[166]. A sub-picosecond hot hole transfer from a gold nanocluster to a GaN slab has been found using similar NAMD techniques[167]. The net hot holes transfer from the metal to the semiconductor, occurring in a subpicosecond scale, is followed by a back-flow of carriers toward the metal species. The authors suggest that such back-flow could be controlled by applying an external potential that modified the Schottky barrier, or by interposing another species such as ZnO between the metal and the semiconductor. A slower, indirect charge transfer mechanism concerns the photoinduced electron injection from Au nanorods to MoS_2, as shown in ref. 168. In this case a fast (30 fs) LSPR decay in HCs pairs within the Au nanorod is followed by a subsequent transfer to the MoS_2 within 100 fs. The relaxation due to e-ph interaction would not show its effect before 200 fs. To rationalize the results of the Au cluster-TiO_2 interface (direct charge transfer) and those of the Au nanorods-MoS_2 ones (indirect charge transfer) it was argued that the specific character of the charge transfer could be ascribed to the degree of coupling between the NP and the semiconductor[168]. The FSSH technique has also been used to study the effect of Sn substitution on hot electrons lifetime in Pt nanoclusters-semiconductor devices[169], and was useful to introduce a new mechanism for energy transfer from a Au plasmonic layer to a semiconductive substrate in which the overlap between the electronic wavefunctions of the two materials allow the transfer of energy without effective charge transfer[170]. rt-TDDFT coupled with FSSH NAMD has also been used to investigate CO_2 photoreduction on rutile TiO_2(110) showing an important interplay between electronic and nuclear degrees of freedom: the excitation of specific vibrational modes stabilizes the CO_2 LUMO which can then trap photoexcited electrons coming from the substrate so that CO_2 gets reduced[171]. This step, which typically takes place spontaneously on transition metal surfaces[172], is prodromal to further reduction steps leading to the synthesis of small hydrocarbons and thus to a sustainable and effective CO_2 recycling process[26,173,174].

Increasing the size of the system

As mentioned in the section "A challenging problem", the main challenges in the simulation of HCs mediated processes in hybrid NP-molecular systems arise from the combination of different length and time scales, and from the variety of phenomena that are involved. While the molecular system, the interface region, the charge transfer, and excitation (at least concerning the molecular part) require atomistic quantum-mechanical treatment in the Å length scale, the typical dimensions of plasmonic NPs are within the 10-100 nm range and can reach even the μm[175,176]. To enlarge the size of the simulated systems while maintaining the computational feasibility, two possible routes are available: using a lower level of approximations of the whole system or using multiscale approaches[177]. Following the first route, approximations to the kinetic term of the standard TDDFT approaches lead to an orbital-free formulation of TDDFT which has been applied to Na NPs with diameter up to 12.3 nm[178], Na NPs dimers and trimers[179], and to Na nanorods[180]. All these studies showed non-trivial behaviors upon bridging the quantum and classical regimes: for instance the sodium NPs absorption spectra would alternately blue shift, red shift and blue shift again upon size decrease as shown in Fig. 5a[178]. Another way to make TDDFT calculations more affordable is to exploit the tight-binding

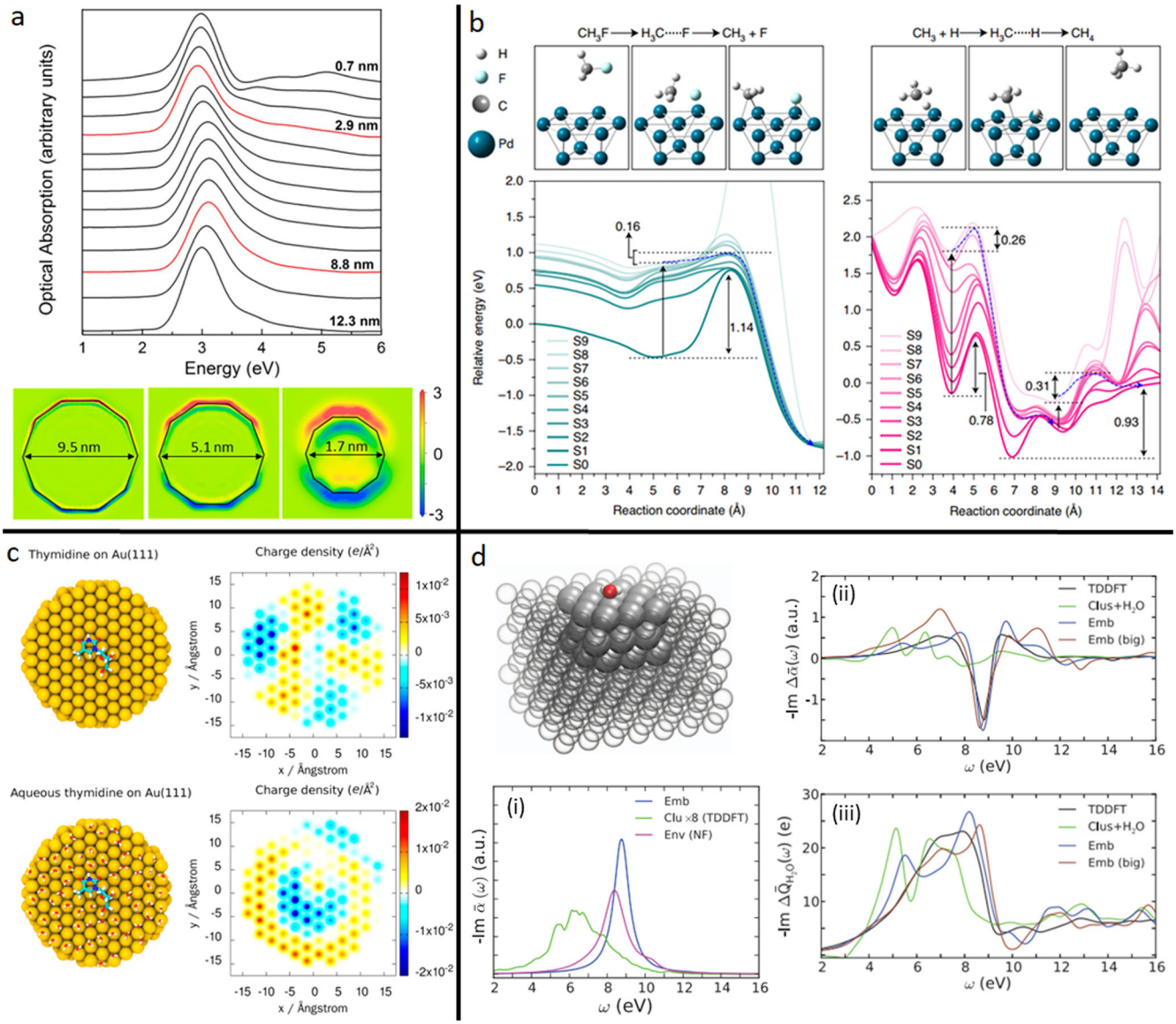

Fig. 5 | Examples of results obtained using tight-binding and multiscale models. **a** Top: Optical absorption spectra of Na NPs which sizes range between 0.7 and 12.3 nm, calculated at the orbital-free TDDFT level. Bottom: Color map of the induced charge densities upon excitation of the Na NPs at the LSPR frequency. Adapted with permission from ref. 178 Copyright 2014 ACS. **b** Scheme of dissociative adsorption of CH_3F (left side) and associative desorption of CH_4 (right side) on a Pd surface, with relative ground-state (S0) and excited-state (S1-S9) potential energy surfaces. Reaction schemes depict reactant, transition-state and product geometries. Possible electronic transitions are marked with vertical arrows while possible trajectories on the potential energy surfaces, calculated with an ECW approach, are marked with blue dashed lines. Adapted with permission from ref. 199 Copyright 2020 Springer Nature. **c** Geometrical configuration and charge distributions of thymidine on Au(111) in vacuum (top) and in a water (bottom). Calculations are performed using a hybrid QM/MM approach based on DFT. Adapted with permission from ref. 209 Copyright 2014 ACS. **d** Graphical representation of the embedding scheme used to simulate the property of a water molecule on top of a Mg slab. Solid spheres represent the part of the system treated at higher theoretical sophistication. (i) Absorption spectra of the free cluster (clu-TDDFT) compared with the one embedded in dielectric environment (env-NF). (ii) Difference in absorption coefficient between H_2O adsorbed and Mg pristine surface. (iii) amount of charge transferred to H_2O. These latter plots compare data obtained with different methods including full TDDFT treatment of the system and embedded approaches, with quantum region being gradually enlarged. Adapted with permission from ref. 224 Copyright 2013 American Physical Society.

approach in which the Kohn-Sham functional is expanded up to the second order around a reference density given by the neutral atoms, and charge fluctuations are decomposed and approximated in atom-centered monopolar contributions[181]. This method has been used to study the generation of HCs in noble metal nanoclusters and nanoalloys[65,182,183], extending the possible size of the systems beyond 30 nm[183,184]. and, when applied to study the properties of metallic structures based on alkaline-metals elements, revealed that, upon excitation, Mg nanoclusters can produce high energetic carriers, suggesting important consequences in chemical processes such as hydrogen evolution[185]. With this level of theory it was possible to study the H_2 photodissociation dynamics over Au and Ag octahedral nanostructures with sizes up to 2.2 nm, elucidating also how the nature of the optical excitations affects the photocatalytic outcome. In particular the authors found that in Au NPs, interband excitations are more effective than LSPR to promote the H_2 cleavage, while the opposite holds for Ag NPs[186]. Interestingly, the authors found the same size-dependance energy trend for the sp and d nature of the optical excitations as in ref. 187. Charge separation at the NP-semiconductor interface has been also investigate with tight-binding TDDFT[188]. This case is particularly interesting as it partially revises previous results obtained on the very same system (Au NP over a TiO_2 slab) at the TDDFT level[147] and extends the analysis to the photocatalytic consequences of interfacial charge transfer. Here, the authors demonstrate that, upon charge separation, the carriers gets stabilized by purely electronic features preventing charge recombination on short timescales. This gives the transferred carriers enough time to activate specific vibrational modes in adsorbed molecular species, which in turn leads to an easier bond dissociation[188]. Finally, to obtain the spatial resolved energy distribution of HCs that reach the surface of realistic nanostructures (~100 nm), a non-equilibrium scattering in space and energy methodology has been proposed[49]. The method combines probabilistic and stochastic approaches to classical transport in combination with source terms and collision models based on accurate electronic structure and e-ph calculations.

To further increase the size of the system while keeping (or even enhance) the theoretical description of a part of it, multiscale methods, in which different regions are modeled at a different level of theoretical accuracy, can be used[189]. Many of these methodologies offer the opportunity to take into account the presence of an entire NP regardless of its size and shape, revealing how effects and phenomena identified by smaller scale studies might be enhanced or hidden when the whole system is involved. Multi-scale techniques are specifically adapted to study problems requiring high-resolution on a specific part of the system (e.g., where a chemical reaction take place) while explicitly accounting for the effects coming from the environment or from another part of the structure under study. Of course, in order to obtain meaningful results it is mandatory to have a solid rationale that guides the division of the system into the various domains where the different theoretical levels are applied. Moreover, the communication between these regions have to be computationally effective and physically accurate. Extended discussions about these issues are available in the literature, see e.g. ref. 189. As summarized in Table 1, row 5, within multiscale methods there are cases where all regions are treated at the quantum level, either using different system modeling (jellium or atomistic) or different approximations for the quantum problem (e.g., DFT or wavefunction based methods), leading to the so-called QM/QM approaches. In other cases, the system is partitioned in a quantum and a classical region using either discrete, QM/MM methods summarized in row 5 of Table 1, or continuum models QM/continuum methods (Table 1, row 6). Employing different modeling of the two subsystems, hot electrons transfer from metallic NPs approximated as jellium medium, to molecules treated atomistically, has been studied using rt-TDDFT coupled to Ehrenfest dynamics[24]. This allowed fundamental insights on the H_2 dissociation process at the metallic NP surface. The study highlighted the importance of the hybridization of the molecular and NP orbitals and of the specific energy level alignment; resulting in a net charge transfer between the NP and the H_2 antibonding orbitals. The magnitude of the charge transfer strongly depends on the NP-molecule distance and, interestingly, in a dimer geometry, the photocatalytic effect is suppressed when the H_2 molecule is located exactly in between the two NPs, due to rapid population and subsequent depopulation of the H_2 antibonding orbital. Water splitting reaction on Au NP has been also investigated using a similar computational approach[190]. By looking at the time evolution of O-H bonds, the study showed how the rate of the reaction depends on the specific plasmonic mode that is excited, suggesting a reaction mechanism that involves the destabilization of the O-H bond through the population of water antibonding orbitals as the LSPR decays, in a time window of 10–20 fs. In 2021, Huang et al. provided further insights on the plasmon-driven water splitting by Au_{20} nanostructures[191]. In this case, the rt-TDDFT and Ehrenfest dynamics of an Au_{20} nanocluster interacting with an H_2O molecule was carried out under the influence of an external laser field and of the near field of a nanosized tetrahedron obtained by classical finite-difference time-domain numerical solution of Maxwell's equations. This study showed the dependence of the reaction rate on the NP size, incident light frequency and intensity, and near-field spatial distribution.

Embedding quantum-quantum multiscale methods have been applied to the description of the ground state[192] and photoinduced phenomena in molecules chemisorbed on plasmonic NPs[193]. In particular, within the Embedded Correlated Wavefunction (ECW) method[74,193] the sensitive portion of the system (i.e. metallic cluster together with adsorbate molecule) is treated at a high level of theory in the presence of an embedding potential obtained through a DFT ground state calculation, and properly accounting for the environment. ECW has been used to study the influence of the metal-adsorbate interface on plasmon damping[102] and photocatalytic processes such as H_2 dissociation on Al NPs[194], H desorption from a Pd surface[195], ammonia decomposition on Cu NPs[196] and Cu-Ru alloyed antenna-reactor systems[197], methane dry reforming on Cu-Ru antenna-reactor system[198], and the activation of carbon-fluorine bonds, as visible from Fig. 5b[199]. The ECW method allows the estimation of excited states activation energies by accurately computing excited states along the geometries of the ground state reaction pathway. Indeed a reduction of the effective barrier upon optical excitation has been found for both H desorption[195] (for which also vibrational excitation seem to play an important role[200]) and ammonia decomposition on Cu NPs[196]. No charge transfers has been detected in these cases whereas it emerged in H_2 decomposition on Al NPs[194]. In the case of NH_3 decomposition on the Cu-Ru system, the rate-determining step for the excited state pathway is different than the one of the ground state reaction[197]. Recently, the very same reactions have been investigated using a similar computational approach also on antenna-reactor systems that use as catalytic centers Fe and Pd nanodisks[201].

Within current implementations of the ECW approach, the embedding potential is computed once for all at the ground state DFT level. A dynamic coupling and feedback between subsystems is instead included in most QM/MM and QM/Continuum methods where the NP is either treated classically as a continuous body or as a discrete system using a MM force field[202–204]. These methods accurately capture how excitation energies, optical and spectroscopic properties of molecules are affected by the presence of plasmonic NPs even for atomic scale protrusions[205–207] and for complex environments including solvents[204,208–210]. However, within the classical region, electrons are not explicitly taken into account. This limitation does not allow the application of these methods to study molecules chemisorbed on the NP surface, charge transfer excitations, and transport phenomena between NPs and molecular species, unless at least a portion of the NP is included in the quantum region. When polarizable QM/MM techniques pair a TDDFT description of the molecule with a classical atomistic representation of the metal NP, it is possible to simulate NPs made of 10^5–10^6 atoms[211]. This approach has been used to look at the optical properties of rhodamine-6G and crystal violet adsorbed on silver and gold NPs[212], at the study of surface-enhanced Raman scattering spectra for pyridine adsorbed on different sites of icosahedral NPs with diameters between 1 and 8 nm[213], and at the investigation of the optical response of thymidine absorbed on gold surfaces in an aqueous environment, as show in Fig. 5c [214].

PCM, originally designed to describe solvent effects, has recently been adapted to model plasmonic NPs in the proximity of a system treated at a quantum level, within a QM/continuum approach[202]. PCM combined with time-dependent HF and TDDFT in the frequency domain allowed to the study of excitation energies of formaldehyde and merocyanine[215] and of fluorescence enhancements of molecules on NPs[205,216]. A continuum description of the plasmonic NP combined with many-body Green's function approach provided a microscopic theory of plasmon-enhanced spectroscopies which included self-consistently the Coulomb interaction between the NP and the molecule through an additional self-energy term[217–219]. PCM studies on plasmonic NPs were also extended to time domain simulations[220], with the possibility of including the effects of decoherence by environment-induced dephasing[221]. By coupling this approach with a MBPT active space for the quantum system, it was possible to explain the how photoexcitation enhanced the selectivity towards methane formation of CO_2 reduction on Rh nanocubes[222]. Still within QM-continuum approaches, a hybrid quasi-static finite-difference time-domain model coupled with TDDFT, suggested the importance of the dynamic coupling between the classical and quantum systems for the description of the spectral changes and enhanced photoabsorption of a Na dimer between two metallic NPs[223]. As depicted in Fig. 5d, rt-TDDFT coupled to classical near field electrodynamics allowed to study the dynamical charge transfer between H_2O molecule and Mg(0001) slab where a small portion of the Mg slab and the water molecule were treated quantum-mechanically[224]. Continuous and classical atomistic models have been used also concurrently. For example a multiscale approach combining PCM, MM and TDDFT allowed to study the LH2 light-harvesting pigment of purple bacteria in protein environment and in proximity of tip-shaped gold NPs[225] and gold nanorods[226]; similarly the light harvesting process of the peridinin-chlorophyll-protein complex on a silver island film has been studied revealing the best geometries and shapes for the optimization of the fluorescence enhancement.

Perspectives

Developing theoretical tools able to capture and predict the behavior of HCs given a specific combination of metallic NP, molecular species and/or semiconductor, and external electromagnetic radiation, lead to the great amount of theoretical and computational work that this review tries to put together and rationalize. Given the complexity of the problem much has still to be done in order to be able to go beyond qualitative descriptions and become quantitatively predictive. Jellium models have provided and still provide basic understandings on the physics behind HC generation and its dependence on particle size and shape; the specific material dependence of the process, especially important to describe the interaction between NP and molecule are naturally introduced relying on DFT-based methodologies. Such ab-initio approaches provided insights on the mechanisms behind HCs generation, transport and injection, allowing remarkable advancements of the discipline. However, DFT-based techniques rely on approximated kernels to tackle the electron correlation and this, in turn, affects the computational predictions especially when dealing with systems where the relative alignment of electronic levels and charge transfer phenomena have a primary importance[74]. In this view, finding ways to implement more sophisticated theories (such as MBPT[94]) without increasing too much the computational cost and/or coupling them with multiscale[189] or embedding approaches could be extremely fruitful. Particularly promising are also the novel real-time non-equilibrium Green's function formulations[227], that include e-ph and e-e scattering at the first principle level. Indeed understanding and describing the coupling between HCs and nuclear degrees of freedom is extremely important, not only to monitor the onset of the chemical reaction but also to address the relationship between improved catalytic performance and system temperature, the interplay between chemical species and NP phonons[228], and the role of inelastic electron-vibrational scattering[200]. In this case, to simulate realistic conditions, further developments and applications of multiscale approaches coupled to NAMDs simulations are highly desirable[229,230]. Theoretical investigation on plasmon-induced photochemistry could also benefit of the novel developments concerning NAMDs simulations themselves like trajectory-based methods, that avoid the calculation of electronic potential energy surfaces and non-adiabatic couplings[231], or spin mapping approaches[232]. Moreover a richer physics could be grasped using recent developments that bridge quantum optics and condensed matter, accounting explicitly for the mutual interaction between electrons, nuclei and photons beyond the *standard* light-matter coupling approaches[233–236]. These novel strategies would provide an even more comprehensive view to the field and include novel phenomena, such as polaritonic-driven dynamics and chemistry[237].

To date, countless experimental studies have shown how plasmon-mediated photocatalysis has the potential to radically transform the chemical industry, allowing high-efficiency production of compounds such as NH_3 from atmospheric nitrogen[238], or H_2 via water splitting[239]. In addition, these type of processes are already being used to convert CO_2 into more versatile chemicals and fuels[26], and in other reactions that can significantly contribute to mitigate the impact of climate change in the coming years[240,241]. In this view, great insights on the origin of the photocatalytic activity of plasmonic NPs have been provided by embedding multiscale methods. Here, further progress could be achieved going beyond a static embedding and/or using MBPT, instead of high level theoretical chemistry methods for the sensitive portion of the system, allowing to enlarge it without losing accuracy[242]. However, not only length scales, but also time scales strongly vary in this class of phenomena. Therefore coupled multiscale methodologies encompassing different time scales should be developed to monitor the evolution of the system from the light pulse to the chemical reactions. As we tried to highlight in this review, to date there is still no a *universal* modeling approach, i.e., a technique able to consider all the complexity and multitude physical effects emerging when light interacts with hybrid NP-molecule systems. However, this does not imply that there are no valuable tools to study these systems in detail. Each of the existing modeling approaches have their own peculiarities which make them suitable to investigate certain specific phenomena. Jellium models, for example, are best suited to understand how the opto-electronic properties of a system depend on the morphology (size, geometry, chemical ordering etc.) of the NP, but they are insufficient to predict reaction mechanisms. On the other hand, ab-initio approaches can elucidate the role of the local atomistic structure in the various HCs life stages and in the formation/destruction of chemical bonds, but they cannot explicitly account for long-range effects coming from the NP extended structure or from the environment. Given their multi-domain nature, multiscale models seem to be a viable solution to combine the advantages of the mentioned methods, and yet they are not exempt from complications. Indeed, approximating the physics of different regions with different levels of theoretical sophistication is extremely delicate as the criterion adopt to set the boundaries has a huge impact on the quality of the model. Further advances of theoretical and computational techniques towards the description of plasmonic-related phenomena will also necessarily deal with the new trends and evidences coming from the experimental progresses. Indeed, in recent years, important advances have been made in the design of efficient composite nanomaterials[163,243,244], exotic-shaped nanostructures[245,246], and non-trivial NPs arrangements[247] such as so-called antenna-reactor systems[198,201,248]. Huge advances have been recently reached in monitoring carrier dynamics[75,249], exploiting the gaps between NPs to activate polaritonic effects[250–253], increasing the efficiency of NP-to-semiconductor charge transfer[254] and using HCs production and transfer as core mechanism for photodetectors[255]. It is worth mentioning also the massive development of the field of chiral plasmonics, which allow to use of external light pulse polarization as a driving force to control HCs production and dynamics and thus to perform photocatalysis[33,256–261]. All these experimental advancements poses new and exciting challenges that we believe are going to stimulate novel developments in modeling and predicting plasmonic-based phenomena, and will eventually be supported by the application of frontiers technologies such as machine learning and artificial intelligence[262].

Received: 7 March 2024; Accepted: 27 August 2024;
Published online: 17 September 2024

References

1. Maier, S. A. *Plasmonics: Fundamentals and Applications* (Springer US, 2007).
2. Alvarez-Puebla, R. A., Li, J. F. & Ling, X. Y. Introduction to advances in plasmonics and its applications. *Nanoscale* **13**, 5935 (2021).
3. Barbillon, G. Plasmonics and its applications. *Materials* **12**, 1502 (2019).
4. Cortés, E. et al. Challenges in plasmonic catalysis. *ACS Nano* **14**, 16202 (2020).
5. Kravets, V. G., Kabashin, A. V., Barnes, W. L. & Grigorenko, A. N. Plasmonic surface lattice resonances: a review of properties and applications. *Chem. Rev.* **118**, 5912 (2018).
6. Yu, H., Peng, Y., Yang, Y. & Li, Z. Y. Plasmon-enhanced light-matter interactions and applications. *npj Comput. Mater.* **5**, 45 (2019).
7. Gieseking, R. L. Plasmons: Untangling the classical, experimental, and quantum mechanical definitions. *Mater. Horiz.* **9**, 25 (2022).
8. Koya, A. N. et al. Advances in ultrafast plasmonics. *Appl. Phys. Rev.* **10**, 021318 (2023).
9. Gieseking, R. L., Ratner, M. A., & Schatz, G. C. *Frontiers of Plasmon Enhanced Spectroscopy.* Vol. 1, Chap. 1, pp. 1–22 (American Chemical Society 2016).
10. Sánchez, C. G. & Berdakin, M. Plasmon-induced hot carriers: an atomistic perspective of the first tens of femtoseconds. *J. Phys. Chem. C* **126**, 10015 (2022).
11. Brongersma, M. L., Halas, N. J. & Nordlander, P. Plasmon-induced hot carrier science and technology. *Nat. Nanotechnol.* **10**, 25 (2015).
12. Li, Z. & Kurouski, D. Plasmon-driven chemistry on mono- and bimetallic nanostructures. *Acc. Chem. Res.* **54**, 2477 (2021).
13. Tang, H. et al. Plasmonic hot electrons for sensing, photodetection, and solar energy applications: A perspective. *J. Chem. Phys.* **152**, 220901 (2020).
14. Hegde, R. S. & Khatua, S. *Nanoelectronics, Advanced Nanomaterials* (ed. Kaushik, B. K.) pp. 289–315 (Elsevier, 2019).
15. Jang, Y. H. et al. Plasmonic solar cells: from rational design to mechanism overview. *Chem. Rev.* **116**, 14982 (2016).
16. Zhan, C. et al. From plasmon-enhanced molecular spectroscopy to plasmon-mediated chemical reactions. *Nat. Rev. Chem.* **2**, 216 (2018).
17. Wei, Q., Wu, S. & Sun, Y. Quantum-sized metal catalysts for hot-electron-driven chemical transformation. *Adv. Mater.* **30**, 1802082 (2018).
18. Kim, M., Lin, M., Son, J., Xu, H. & Nam, J. M. Hot-electron-mediated photochemical reactions: Principles, recent advances, and challenges. *Adv. Opt. Mater.* **5**, 1700004 (2017).
19. Swearer, D. F. et al. Heterometallic antenna-reactor complexes for photocatalysis. *Proc. Natl Acad. Sci. USA* **113**, 8916 (2016).
20. Zhan, C. et al. Plasmon-mediated chemical reactions. *Nat. Rev. Methods Prim.* **3**, 12 (2023).
21. Zhang, Y. et al. Plasmon-mediated photodecomposition of NH3 via intramolecular charge transfer. *Nano Res.* **15**, 3894 (2022).
22. Narang, P., Sundararaman, R. & Atwater, H. A. Plasmonic hot carrier dynamics in solid-state and chemical systems for energy conversion. *Nanophotonics* **5**, 96 (2016).
23. Aslam, U., Rao, V. G., Chavez, S. & Linic, S. Catalytic conversion of solar to chemical energy on plasmonic metal nanostructures. *Nat. Catal.* **1**, 656 (2018).
24. Zhang, Y., Nelson, T. R., Tretiak, S., Guo, H. & Schatz, G. C. Plasmonic hot-carrier mediated tunable photochemical reactions. *ACS Nano* **12**, 8415 (2018).
25. Choi, C. H., Chung, K., Nguyen, T. T. & Kim, D. H. Plasmon-mediated electrocatalysis for sustainable energy: from electrochemical conversion of different feedstocks to fuel cell reactions. *ACS Energy Lett.* **3**, 1415 (2018).
26. Verma, R., Belgamwar, R. & Polshettiwar, V. Plasmonic photocatalysis for CO2 conversion to chemicals and fuels. *ACS Mater. Lett.* **3**, 574 (2021).
27. Ciocarlan, R. G., Blommaerts, N., Lenaerts, S., Cool, P. & Verbruggen, S. W. Recent trends in plasmon-assisted photocatalytic CO2 reduction. *ChemSusChem* **16**, e202201647 (2023).
28. Hu, C. et al. Near-infrared-featured broadband CO2 reduction with water to hydrocarbons by surface plasmon. *Nat. Commun.* **14**, 221 (2023).
29. Mittal, D., Ahlawat, M. & Govind Rao, V. Recent progress and challenges in plasmon-mediated reduction of CO2 to chemicals and fuels. *Adv. Mater. Interfaces* **9**, 2102383 (2022).
30. Zhang, Y. et al. Indirect to direct charge transfer transition in plasmon-enabled CO2 photoreduction. *Adv. Sci.* **9**, 2102978 (2022).
31. Cortés, E. Efficiency and bond selectivity in plasmon-induced photochemistry. *Adv. Opt. Mater.* **5**, 1700191 (2017).
32. Zhang, X., Ke, X. & Yao, J. Recent development of plasmon-mediated photocatalysts and their potential in selectivity regulation. *J. Mater. Chem. A* **6**, 1941 (2018).
33. Negrín-Montecelo, Y. et al. Synergistic combination of charge carriers and energy-transfer processes in plasmonic photocatalysis. *ACS Appl. Mater. Interfaces* **14**, 35734 (2022).
34. Zhou, L. et al. Quantifying hot carrier and thermal contributions in plasmonic photocatalysis. *Science* **362**, 69 (2018).
35. Linic, S., Chavez, S. & Elias, R. Flow and extraction of energy and charge carriers in hybrid plasmonic nanostructures. *Nat. Mater.* **20**, 916–924 (2021).
36. Sivan, Y. & Dubi, Y. Recent developments in plasmon-assisted photocatalysis - a personal perspective. *Appl. Phys. Lett.* **117**, 130501 (2020).
37. Jain, P. K. Taking the heat off of plasmonic chemistry. *J. Phys. Chem. C* **123**, 24347 (2019).
38. Zhang, J. et al. Regulation of energetic hot carriers on Pt/TiO2 with thermal energy for photothermal catalysis. *Appl. Catal. B: Environ.* **309**, 121263 (2022).
39. Geng, Z., Yu, Y. & Liu, J. Broadband plasmonic photocatalysis enhanced by photothermal light absorbers. *J. Phys. Chem. C* **127**, 17723 (2023).
40. Baumberg, J. J. Hot electron science in plasmonics and catalysis: what we argue about. *Faraday Discuss.* **214**, 501 (2019).
41. Wu, S. & Sheldon, M. Mechanisms of photothermalization in plasmonic nanostructures: Insights into the steady state. *Annu. Rev. Phys. Chem.* **74**, 521 (2023).
42. Carlin, C. C. et al. Nanoscale and ultrafast in situ techniques to probe plasmon photocatalysis. *Chem. Phys. Rev.* **4**, 041309 (2023).
43. Chen, X., Liu, P. & Jensen, L. Atomistic electrodynamics simulations of plasmonic nanoparticles. *J. Phys. D: Appl. Phys.* **52**, 363002 (2019).
44. Newmeyer, E. R., North, J. D. & Swearer, D. F. Hot carrier photochemistry on metal nanoparticles. *J. Appl. Phys.* **132**, 230901 (2022).
45. Maurer, R. J. & Jain, P. K. Hot electrons in catalysis. *J. Phys. Chem. C* **128**, 1863 (2024).
46. Weight, B. M., Li, X. & Zhang, Y. Theory and modeling of light-matter interactions in chemistry: current and future. *Phys. Chem. Chem. Phys.* **25**, 31554 (2023).
47. Schirato, A., Maiuri, M., Cerullo, G. & Della Valle, G. Ultrafast hot electron dynamics in plasmonic nanostructures: experiments, modelling, design. *Nanophotonics* **12**, 1 (2023).
48. Brown, A. M. et al. Experimental and ab initio ultrafast carrier dynamics in plasmonic nanoparticles. *Phys. Rev. Lett.* **118**, 087401 (2017).

49. Jermyn, A. S. et al. Transport of hot carriers in plasmonic nanostructures. *Phys. Rev. Mater.* **3**, 075201 (2019).
50. Burke, K. & Wagner, L. O. Dft in a nutshell. *Int. J. Quant. Chem.* **113**, 96 (2013).
51. Reining, L. The GW approximation: content, successes and limitations. *WIREs Comput. Mol. Sci.* **8**, e1344 (2018).
52. Schirato, A., Crotti, G., Proietti Zaccaria, R., Alabastri, A. & Della Valle, G. Hot carrier spatio-temporal inhomogeneities in ultrafast nanophotonics. *N. J. Phys.* **24**, 045001 (2022).
53. Amirjani, A. & Sadrnezhaad, S. K. Computational electromagnetics in plasmonic nanostructures. *J. Mater. Chem. C* **9**, 9791 (2021).
54. Wokaun, A., Gordon, J. P. & Liao, P. F. Radiation damping in surface-enhanced raman scattering. *Phys. Rev. Lett.* **48**, 957 (1982).
55. Varnavski, O. P., Mohamed, M. B., El-Sayed, M. A. & Goodson, T. Relative enhancement of ultrafast emission in gold nanorods. *J. Phys. Chem. B* **107**, 3101 (2003).
56. Dulkeith, E. et al. Plasmon emission in photoexcited gold nanoparticles. *Phys. Rev. B* **70**, 205424 (2004).
57. Mittal, R., Glenn, R., Saytashev, I., Lozovoy, V. V. & Dantus, M. Femtosecond nanoplasmonic dephasing of individual silver nanoparticles and small clusters. *J. Phys. Chem. Lett.* **6**, 1638 (2015).
58. Khurgin, J. B. Hot carriers generated by plasmons: where are they generated and where do they go from there? *Faraday Discuss.* **214**, 35 (2019).
59. Fregoni, J., Garcia-Vidal, F. J. & Feist, J. Theoretical challenges in polaritonic chemistry. *ACS Photon.* **9**, 1096 (2022).
60. Bernardi, M., Mustafa, J., Neaton, J. B. & Louie, S. G. Theory and computation of hot carriers generated by surface plasmon polaritons in noble metals. *Nat. Commun.* **6**, 7044 (2015).
61. Thakkar, N., Montoni, N. P., Cherqui, C. & Masiello, D. J. Plasmonic landau damping in active environments. *Phys. Rev. B* **97**, 121403 (2018).
62. Manjavacas, A., Liu, J. G., Kulkarni, V. & Nordlander, P. Plasmon-induced hot carriers in metallic nanoparticles. *ACS Nano* **8**, 7630 (2014).
63. Romanelli, M. et al. Effective single-mode methodology for strongly coupled multimode molecular-plasmon nanosystems. *Nano Lett.* **23**, 4938 (2023).
64. Rossi, T. P., Erhart, P. & Kuisma, M. Hot-carrier generation in plasmonic nanoparticles: the importance of atomic structure. *ACS Nano* **14**, 9963 (2020).
65. Douglas-Gallardo, O. A., Berdakin, M., Frauenheim, T. & Sánchez, C. G. Plasmon-induced hot-carrier generation differences in gold and silver nanoclusters. *Nanoscale* **11**, 8604 (2019).
66. Christopher, P. & Moskovits, M. Hot charge carrier transmission from plasmonic nanostructures. *Annu. Rev. Phys. Chem.* **68**, 379 (2017).
67. Chang, L. et al. Electronic structure of the plasmons in metal nanocrystals: fundamental limitations for the energy efficiency of hot electron generation. *ACS Energy Lett.* **4**, 2552 (2019).
68. Cunha, J. et al. Controlling light, heat, and vibrations in plasmonics and phononics. *Adv. Opt.Mater.* **8**, 2001225 (2020).
69. Neukirch, A. J., Guo, Z. & Prezhdo, O. V. Time-domain ab initio study of phonon-induced relaxation of plasmon excitations in a silver quantum dot. *J. Phys. Chem. C* **116**, 15034 (2012).
70. Reddy, H. & Shalaev, V. M. Plasmonic hot-carriers and their applications: opinion. *Opt. Mater. Express* **11**, 3827 (2021).
71. Dong, Y., Hu, C., Xiong, H., Long, R. & Xiong, Y. Plasmonic catalysis: new opportunity for selective chemical bond evolution. *ACS Catal.* **13**, 6730 (2023).
72. Jain, V., Kashyap, R. K. & Pillai, P. P. Plasmonic photocatalysis: activating chemical bonds through light and plasmon. *Adv. Opt. Mater.* **10**, 2200463 (2022).
73. Lee, S. W. Hot electron-driven chemical reactions: a review. *Appl. Surf. Sci. Adv.* **16**, 100428 (2023).
74. Martirez, J. M. P., Bao, J. L. & Carter, E. A. First-principles insights into plasmon-induced catalysis. *Annu. Rev. Phys. Chem.* **72**, 99 (2021).
75. Pettine, J. & Nesbitt, D. J. Emerging methods for controlling hot carrier excitation and emission distributions in nanoplasmonic systems. *J. Phys. Chem. C* **126**, 14767 (2022).
76. Dal Forno, S., Ranno, L. & Lischner, J. Material, size, and environment dependence of plasmon-induced hot carriers in metallic nanoparticles. *J. Phys. Chem. C* **122**, 8517 (2018).
77. Ranno, L., Forno, S. D. & Lischner, J. Computational design of bimetallic core-shell nanoparticles for hot-carrier photocatalysis. *npj Comput. Mater.* **4**, 31 (2018).
78. Kumarasinghe, C. S., Premaratne, M., Bao, Q. & Agrawal, G. P. Theoretical analysis of hot electron dynamics in nanorods. *Sci. Rep.* **5**, 12140 (2015).
79. Govorov, A. O., Zhang, H. & Gun'ko, Y. K. Theory of photoinjection of hot plasmonic carriers from metal nanostructures into semiconductors and surface molecules. *J. Phys. Chem. C* **117**, 16616 (2013).
80. Zhang, H. & Govorov, A. O. Optical generation of hot plasmonic carriers in metal nanocrystals: the effects of shape and field enhancement. *J. Phys. Chem. C* **118**, 7606 (2014).
81. Besteiro, L. & Govorov, A. O. Amplified generation of hot electrons and quantum surface effects in nanoparticle dimers with plasmonic hot spots. *J. Phys. Chem. C* **120**, 19329 (2016).
82. Naik, G. V. & Dionne, J. A. Photon upconversion with hot carriers in plasmonic systems. *Appl. Phys. Lett.* **107**, 133902 (2015).
83. Besteiro, L. V., Kong, X. T., Wang, Z., Hartland, G. & Govorov, A. O. Understanding hot-electron generation and plasmon relaxation in metal nanocrystals: quantum and classical mechanisms. *ACS Photon.* **4**, 2759 (2017).
84. Kong, X. T., Wang, Z. & Govorov, A. O. Plasmonic nanostars with hot spots for efficient generation of hot electrons under solar illumination. *Adv. Opt. Mater.* **5**, 1600594 (2017).
85. Santiago, E. Y. et al. Efficiency of hot-electron generation in plasmonic nanocrystals with complex shapes: surface-induced scattering, hot spots, and interband transitions. *ACS Photon.* **7**, 2807 (2020).
86. Saavedra, J. R. M., Asenjo-Garcia, A. & García de Abajo, F. J. Hot-electron dynamics and thermalization in small metallic nanoparticles. *ACS Photon.* **3**, 1637 (2016).
87. Liu, J. G., Zhang, H., Link, S. & Nordlander, P. Relaxation of plasmon-induced hot carriers. *ACS Photon.* **5**, 2584 (2018).
88. Zhang, Y. Theory of plasmonic hot-carrier generation and relaxation. *J. Phys. Chem. A* **125**, 9201 (2021).
89. Song, P., Nordlander, P. & Gao, S. Quantum mechanical study of the coupling of plasmon excitations to atomic-scale electron transport. *J. Chem. Phys.* **134**, 074701 (2011).
90. Kulkarni, V. & Manjavacas, A. Quantum effects in charge transfer plasmons. *ACS Photon.* **2**, 987 (2015).
91. Gao, S. Nonlinear response of metal nanoparticles: double plasmon excitation and electron transfer. *J. Chem. Phys.* **142**, 234701 (2015).
92. Hess, O., Lischner, J. & Castellanos, L. R. Dielectric engineering of hot-carrier generation by quantized plasmons in embedded silver nanoparticles. *J. Phys. Chem. C* **125**, 3081 (2021).
93. Crai, A. et al. Coulomb effects on the photoexcited quantum dynamics of electrons in a plasmonic nanosphere. *Phys. Rev. B* **98**, 165411 (2018).
94. Onida, G., Reining, L. & Rubio, A. Electronic excitations: density-functional versus many-body green's-function approaches. *Rev. Mod. Phys.* **74**, 601 (2002).
95. Quijada, M., Muiño, R. D., Borisov, A. G., Alonso, J. A. & Echenique, P. M. Lifetime of electronic excitations in metal nanoparticles. *N. J. Phys.* **12**, 053023 (2010).

96. Román Castellanos, L., Hess, O. & Lischner, J. Single plasmon hot carrier generation in metallic nanoparticles. *Commun. Phys.* **2**, 47 (2019).
97. Varas, A., García-González, P., Feist, J., García-Vidal, F. & Rubio, A. Quantum plasmonics: from jellium models to ab ini- tio calculations. *Nanophotonics* **5**, 409 (2016).
98. Zhang, P., Feist, J., Rubio, A., García-González, P. & García-Vidal, F. J. Ab initio nanoplasmonics: the impact of atomic structure. *Phys. Rev. B - Condens. Matter Mater. Phys.* **90**, 161407 (2014).
99. Zubizarreta, X. et al. Quantum-size effects in the loss function of Pb(111) thin films: an ab initio study. *Phys. Rev. B* **95**, 235405 (2017).
100. Sundararaman, R., Narang, P., Jermyn, A. S., Goddard III, W. A. & Atwater, H. A. Theoretical predictions for hot-carrier generation from surface plasmon decay. *Nat. Commun.* **5**, 5788 (2014).
101. Kumar, P. V. & Norris, D. J. Tailoring energy transfer from hot electrons to adsorbate vibrations for plasmon-enhanced catalysis. *ACS Catal.* **7**, 8343 (2017).
102. Foerster, B., Spata, V. A., Carter, E. A., Sönnichsen, C. & Link, S. Plasmon damping depends on the chemical nature of the nanoparticle interface. *Sci. Adv.* **5**, eaav0704 (2019).
103. Li, W., Xue, T., Mora-Perez, C. & Prezhdo, O. V. Ab initio quantum dynamics of plasmonic charge carriers. *Trends Chem.* **5**, 634 (2023).
104. Seibel, C. et al. Time-resolved spectral densities of nonthermal electrons in gold. *J. Phys. Chem. C* **127**, 23349 (2023).
105. Román Castellanos, L., Kahk, J. M., Hess, O. & Lischner, J. Generation of plasmonic hot carriers from d-bands in metallic nanoparticles. *J. Chem. Phys.* **152**, 104111 (2020).
106. Marzari, N., Mostofi, A. A., Yates, J. R., Souza, I. & Vanderbilt, D. Maximally localized wannier functions: theory and applications. *Rev. Mod. Phys.* **84**, 1419 (2012).
107. Brown, A. M., Sundararaman, R., Narang, P., Goddard, W. A. & Atwater, H. A. Ab initio phonon coupling and optical response of hot electrons in plasmonic metals. *Phys. Rev. B* **94**, 075120 (2016).
108. Brown, A. M., Sundararaman, R., Narang, P., Goddard, W. A. & Atwater, H. A. Nonradiative plasmon decay and hot carrier dynamics: Effects of phonons, surfaces, and geometry. *ACS Nano* **10**, 957 (2016).
109. Habib, A., Florio, F. & Sundararaman, R. Hot carrier dynamics in plasmonic transition metal nitrides. *J. Opt.* **20**, 064001 (2018).
110. Jiang, Y. et al. Enhanced optical response in au nanopillar/ la0.67sr0.33mno3 film composites: Implications for magnetooptical devices. *ACS Appl. Nano Mater.* **6**, 342 (2023).
111. Gaspari, R. et al. Quasi-static resonances in the visible spectrum from all-dielectric intermediate band semiconductor nanocrystals. *Nano Lett.* **17**, 7691 (2017).
112. Zavelani-Rossi, M. et al. Transient optical response of a single gold nanoantenna: the role of plasmon detuning. *ACS Photon.* **2**, 521 (2015).
113. Mou, T., Quiroz, J., Camargo, P. H. & Wang, B. Localized orbital excitation drives bond formation in plasmonic catalysis. *ACS Appl. Mater. Interfaces* **13**, 60115 (2021).
114. Le, T., Shao, Y. & Wang, B. Plasmon-Induced CO2Conversion on Al@Cu2O: a DFT study. *J. Phys. Chem. C* **125**, 6108 (2021).
115. Casida, M. & Huix-Rotllant, M. Progress in time-dependent density-functional theory. *Annu. Rev. Phys. Chem.* **63**, 287 (2012).
116. Casida, M. E. *Recent Advances in Density Functional Methods*, pp. 155–192 (World Scientific Publishing Co Pte Ltd, 1995).
117. O'Rourke, C. & Bowler, D. R. Linear scaling density matrix real time TDDFT: propagator unitarity and matrix truncation. *J. Chem. Phys.* **143**, 102801 (2015).
118. Baseggio, O. et al. Photoabsorption of icosahedral noble metal clusters: An efficient tddft approach to large-scale systems. *J. Phys. Chem. C* **120**, 12773 (2016).
119. Aikens, C. M., Li, S. & Schatz, G. C. From discrete electronic states to plasmons: Tddft optical absorption properties of Agn (n = 10, 20, 35, 56, 84, 120) tetrahedral clusters. *J. Phys. Chem. C* **112**, 11272 (2008).
120. Durante, N., Fortunelli, A., Broyer, M. & Stener, M. Optical properties of Au nanoclusters from TD-DFT calculations. *J. Phys. Chem. C* **115**, 6277 (2011).
121. Bae, G. T. & Aikens, C. M. Time-dependent density functional theory studies of optical properties of au nanoparticles: Octahedra, truncated octahedra, and icosahedra. *J. Phys. Chem. C* **119**, 23127 (2015).
122. Vanzan, M. & Corni, S. Role of organic ligands orientation on the geometrical and optical properties of Au25(SCH3)18. *J. Phys. Chem. A* **122**, 6864 (2018).
123. Zhang, P., Jin, W. & Liang, W. Unveiling the effect of electron tunneling on the plasmonic resonance of closely spaced gold particles. *Phys. Chem. Chem. Phys.* **22**, 1747 (2020).
124. Barcaro, G., Broyer, M., Durante, N., Fortunelli, A. & Stener, M. Alloying effects on the optical properties of Ag-Au nanoclusters from tddft calculations. *J. Phys. Chem. C* **115**, 24085 (2011).
125. Barcaro, G., Sementa, L., Fortunelli, A. & Stener, M. Optical properties of Pt and Ag-Pt nanoclusters from TDDFT calculations: Plasmon suppression by pt poisoning. *J. Phys. Chem. C* **118**, 28101 (2014).
126. Vanzan, M. et al. Lanthanide ions sensitization by small noble metal nanoclusters. *ACS Photon.* **8**, 1364 (2021).
127. Baseggio, O., Vetta, M. D., Fronzoni, G., Stener, M. & Fortunelli, A. A new time-dependent density-functional method for molecular plasmonics: formalism, implementation, and the au144(sh)60 case study. *Int. J. Quant. Chem.* **116**, 1603 (2016).
128. Baseggio, O., Fronzoni, G. & Stener, M. A new time dependent density functional algorithm for large systems and plasmons in metal clusters. *J. Chem. Phys.* **143**, 024106 (2015).
129. Baseggio, O. et al. Time-dependent density-functional study of the photoabsorption spectrum of Au25(SC2H4C6H5)18 anion: Validation of the computational protocol. *Int. J. Quant. Chem.* **118**, e25769 (2018).
130. Sementa, L. et al. Ligand-enhanced optical response of gold nanomolecules and its fragment projection analysis: the case of Au30(SR)18. *J. Phys. Chem. C* **121**, 10832 (2017).
131. Sakthivel, N. A. et al. Au279(sr)84: the smallest gold thiolate nanocrystal that is metallic and the birth of plasmon. *J. Phys. Chem. Lett.* **9**, 1295 (2018).
132. Sakthivel, N. A. et al. The missing link: Au191(sph-tbu)66 janus nanoparticle with molecular and bulk-metal-like properties. *J. Am. Chem. Soc.* **142**, 15799 (2020).
133. Domenis, N. et al. Time evolution of plasmonic features in pentagonal Ag clusters. *Molecules* **28**, 5671 (2023).
134. Li, Z. et al. Role of plasmonic antenna in hot carrier-driven reactions on bimetallic nanostructures. *J. Phys. Chem. C* **127**, 22635 (2023).
135. Xiong, Y. et al. Photodriven catalytic hydrogenation of CO2 to CH4 with nearly 100% selectivity over Ag25 clusters. *Nano Lett.* **21**, 8693 (2021).
136. Rossi, T. P., Kuisma, M., Puska, M. J., Nieminen, R. M. & Erhart, P. Kohn-sham decomposition in real-time time-dependent density-functional theory: an efficient tool for analyzing plasmonic excitations. *J. Chem. Theory Comput.* **13**, 4779 (2017).
137. Tancogne-Dejean, N. et al. Octopus, a computational framework for exploring light-driven phenomena and quantum dynamics in extended and finite systems. *J. Chem. Phys.* **152**, 124119 (2020).
138. Zhang, K. & Zhang, H. Plasmon coupling in gold nanotube assemblies: insight from a time-dependent density functional theory (tddft) calculation. *J. Phys. Chem. C* **118**, 635 (2014).
139. Yin, H., Zhang, H. & Cheng, X. L. Plasmon resonances and the plasmon-induced field enhancement in nanoring dimers. *J. Appl. Phys.* **113**, 113107 (2013).
140. Conley, K. M. et al. Plasmon excitations in mixed metallic nanoarrays. *ACS Nano* **13**, 5344 (2019).

141. Senanayake, R. D., Lingerfelt, D. B., Kuda-Singappulige, G. U., Li, X. & Aikens, C. M. Real-time TDDFT investigation of optical absorption in gold nanowires. *J. Phys. Chem. C* **123**, 14734 (2019).
142. Iida, K., Noda, M., Ishimura, K. & Nobusada, K. First-principles computational visualization of localized surface plasmon resonance in gold nanoclusters. *J. Phys. Chem. A* **118**, 11317 (2014).
143. Kuisma, M. et al. Localized surface plasmon resonance in silver nanoparticles: atomistic first-principles time-dependent density-functional theory calculations. *Phys. Rev. B - Condens. Matter Mater. Phys.* **91**, 115431 (2015).
144. Zhang, P., Jin, W. & Liang, W. Size-dependent optical properties of aluminum nanoparticles: From classical to quantum description. *J. Phys. Chem. C* **122**, 10545 (2018).
145. Ma, J., Wang, Z. & Wang, L. W. Interplay between plasmon and single-particle excitations in a metal nanocluster. *Nat. Commun.* **6**, 10107 (2015).
146. Kumar, P. V. et al. Plasmon-induced direct hot-carrier transfer at metal-acceptor interfaces. *ACS Nano* **13**, 3188 (2019).
147. Ma, J. & Gao, S. Plasmon-induced electron-hole separation at the Ag/TiO2(110) interface. *ACS Nano* **13**, 13658 (2019).
148. Kumar, P. V., Rossi, T. P., Kuisma, M., Erhart, P. & Norris, D. J. Direct hot-carrier transfer in plasmonic catalysis. *Faraday Discuss.* **214**, 189 (2019).
149. Kluczyk-Korch, K. & Antosiewicz, T. J. Hot carrier generation in a strongly coupled molecule-plasmonic nanoparticle system. *Nanophotonics* **12**, 1711 (2023).
150. Fojt, J., Rossi, T. P., Kuisma, M. & Erhart, P. Hot-carrier transfer across a nanoparticle-molecule junction: the importance of orbital hybridization and level alignment. *Nano Lett.* **22**, 8786 (2022).
151. Kuda-Singappulige, G. U., Lingerfelt, D. B., Li, X. & Aikens, C. M. Ultrafast nonlinear plasmon decay processes in silver nanoclusters. *J. Phys. Chem. C* **124**, 20477 (2020).
152. Yan, L., Guan, M. & Meng, S. Plasmon-induced nonlinear response of silver atomic chains. *Nanoscale* **10**, 8600 (2018).
153. Hull, O. A. & Aikens, C. M. Theoretical investigations on the plasmon-mediated dissociation of small molecules in the presence of silver atomic wires. *J. Phys. Chem. A* **127**, 2228 (2023).
154. Vanzan, M., Gil, G., Castaldo, D., Nordlander, P. & Corni, S. Energy transfer to molecular adsorbates by transient hot electron spillover. *Nano Lett.* **23**, 2719 (2023).
155. Wang, Z. et al. Phonon-assisted auger process enables ultrafast charge transfer in cdse quantum dot/organic molecule. *J. Phys. Chem. C* **123**, 17127 (2019).
156. Sivan, Y., Un, I. W. & Dubi, Y. Assistance of metal nanoparticles in photocatalysis-nothing more than a classical heat source. *Faraday Discuss.* **214**, 215 (2019).
157. Dubi, Y., Un, I. W. & Sivan, Y. Thermal effects - an alternative mechanism for plasmon-assisted photocatalysis. *Chem. Sci.* **11**, 5017 (2020).
158. Un, I. W. & Sivan, Y. Parametric study of temperature distribution in plasmon-assisted photocatalysis. *Nanoscale* **12**, 17821 (2020).
159. Hogan, N., Wu, S. & Sheldon, M. Photothermalization and hot electron dynamics in the steady state. *J. Phys. Chem. C* **124**, 4931 (2020).
160. Nelson, T. R. et al. Non-adiabatic excited-state molecular dynamics: theory and applications for modeling photophysics in extended molecular materials. *Chem. Rev.* **120**, 2215 (2020).
161. Yan, L., Xu, J., Wang, F. & Meng, S. Plasmon-induced ultrafast hydrogen production in liquid water. *J. Phys. Chem. Lett.* **9**, 63 (2018).
162. Hull, O. A., Lingerfelt, D. B., Li, X. & Aikens, C. M. Electronic structure and nonadiabatic dynamics of atomic silver nanowire-N2 systems. *J. Phys. Chem. C* **124**, 20834 (2020).
163. Wang, Y. & Aikens, C. M. Connectivity between static field and continuous wave field effects on excitation-induced H2 activation. *J. Phys. Chem. C* **127**, 15375 (2023).
164. Zhang, Y., Chen, D., Meng, W., Li, S. & Meng, S. Plasmon-induced water splitting on Ag-alloyed Pt single-atom catalysts. *Front. Chem.* **9**, 742794 (2021).
165. Long, R. & Prezhdo, O. V. Instantaneous generation of charge-separated state on TiO2 surface sensitized with plasmonic nanoparticles. *J. Am. Chem. Soc.* **136**, 4343 (2014).
166. Zhang, J., Guan, M., Lischner, J., Meng, S. & Prezhdo, O. V. Coexistence of different charge-transfer mechanisms in the hot-carrier dynamics of hybrid plasmonic nanomaterials. *Nano Lett.* **19**, 3187 (2019).
167. Zheng, F. & Wang, L. W. Ultrafast hot carrier injection in au/gan: the role of band bending and the interface band structure. *J. Phys. Chem. Lett.* **10**, 6174 (2019).
168. Zhang, Z. et al. Plasmon-mediated electron injection from au nanorods into MoS2: traditional versus photoexcitation mechanism. *Chem.* **4**, 1112 (2018).
169. Wang, X. & Long, R. Thermal-driven dynamic shape change of bimetallic nanoparticles extends hot electron lifetime of Pt/MoS2 catalysts. *J. Phys. Chem. Lett.* **12**, 7173 (2021).
170. Tomko, J. A. et al. Long-lived modulation of plasmonic absorption by ballistic thermal injection. *Nat. Nanotechnol.* **16**, 47 (2021).
171. Chu, W., Zheng, Q., Prezhdo, O. V. & Zhao, J. CO2 Photoreduction on metal oxide surface is driven by transient capture of hot electrons: Ab initio quantum dynamics simulation. *J. Am. Chem. Soc.* **142**, 3214 (2020).
172. Dai, X. & Sun, Y. Reduction of carbon dioxide on photoexcited nanoparticles of VIII group metals. *Nanoscale* **11**, 16723 (2019).
173. Miao, B., Ma, S. S. K., Wang, X., Su, H. & Chan, S. H. Catalysis mechanisms of CO2 and CO methanation. *Catal. Sci. Technol.* **6**, 4048 (2016).
174. Vanzan, M., Marsili, M. & Corni, S. Study of the rate-determining step of Rh catalyzed CO2 reduction: Insight on the hydrogen assisted molecular dissociation. *Catalysts* **11**, 538 (2021).
175. Jiang, N., Zhuo, X. & Wang, J. Active plasmonics: principles, structures, and applications. *Chem. Rev.* **118**, 3054 (2018).
176. Hernandez, R. et al. Delocalized hot electron generation with propagative surface plasmon polaritons. *ACS Photon.* **6**, 1500 (2019).
177. Coccia, E. et al. Hybrid theoretical models for molecular nanoplasmonics. *J. Chem. Phys.* **153**, 200901 (2020).
178. Xiang, H., Zhang, X., Neuhauser, D. & Lu, G. Size-dependent plasmonic resonances from large-scale quantum simulations. *J. Phys. Chem. Lett.* **5**, 1163 (2014).
179. Xiang, H., Zhang, M., Zhang, X. & Lu, G. Understanding quantum plasmonics from time-dependent orbital-free density functional theory. *J. Phys. Chem. C* **120**, 14330 (2016).
180. Xiang, H., Wang, Z., Xu, L., Zhang, X. & Lu, G. Quantum plasmonics in nanorods: a time-dependent orbital-free density functional theory study with thousands of atoms. *J. Phys. Chem. C* **124**, 945 (2020).
181. Niehaus, T. A. et al. Tight-binding approach to time-dependent density-functional response theory. *Phys. Rev. B* **63**, 085108 (2001).
182. Douglas-Gallardo, O. A., Berdakin, M. & Sánchez, C. G. Atomistic insights into chemical interface damping of surface plasmon excitations in silver nanoclusters. *J. Phys. Chem. C* **120**, 24389 (2016).
183. Jin, H., Herran, M., Cortés, E. & Lischner, J. Theory of hot-carrier generation in bimetallic plasmonic catalysts. *ACS Photon.* **10**, 3629 (2023).
184. Jin, H., Kahk, J. M., Papaconstantopoulos, D. A., Ferreira, A. & Lischner, J. Plasmon-induced hot carriers from interband and intraband transitions in large noble metal nanoparticles. *PRX Energy* **1**, 013006 (2022).
185. Douglas-Gallardo, O. A., Box, C. L. & Maurer, R. J. Plasmonic enhancement of molecular hydrogen dissociation on metallic magnesium nanoclusters. *Nanoscale* **13**, 11058 (2021).

186. Giri, S. K. & Schatz, G. C. Photodissociation of H2 on Ag and Au nanoparticles: effect of size and plasmon versus interband transitions on threshold intensities for dissociation. *J. Phys. Chem. C* **127**, 4115 (2023).
187. Berdakin, M., Douglas-Gallardo, O. A. & Sánchez, C. G. Interplay between intra- and interband transitions associated with the plasmon-induced hot carrier generation process in silver and gold nanoclusters. *J. Phys. Chem. C* **124**, 1631 (2020).
188. Berdakin, M. et al. Dynamical evolution of the schottky barrier as a determinant contribution to electron-hole pair stabilization and photocatalysis of plasmon-induced hot carriers. *Nanoscale* **14**, 2816 (2022).
189. Capone, M. et al. A vision for the future of multiscale modeling. *ACS Phys. Chem. Au* **4**, 202–225 (2024).
190. Yan, L., Wang, F. & Meng, S. Quantum mode selectivity of plasmon-induced water splitting on gold nanoparticles. *ACS Nano* **10**, 5452 (2016).
191. Huang, J., Zhao, X., Huang, X. & Liang, W. Understanding the mechanism of plasmon-driven water splitting: Hot electron injection and a near field enhancement effect. *Phys. Chem. Chem. Phys.* **23**, 25629 (2021).
192. Pal, P. P., Liu, P. & Jensen, L. Polarizable frozen density embedding with external orthogonalization. *J. Chem. Theory Comput.* **15**, 6588 (2019).
193. Libisch, F., Huang, C. & Carter, E. A. Embedded correlated wavefunction schemes: theory and applications. *Acc. Chem. Res.* **47**, 2768 (2014).
194. Zhou, L. et al. Aluminum nanocrystals as a plasmonic photocatalyst for hydrogen dissociation. *Nano Lett.* **16**, 1478 (2016).
195. Spata, V. A. & Carter, E. A. Mechanistic insights into photocatalyzed hydrogen desorption from palladium surfaces assisted by localized surface plasmon resonances. *ACS Nano* **12**, 3512 (2018).
196. Bao, J. L. & Carter, E. A. Surface-plasmon-induced ammonia decomposition on copper: Excited-state reaction pathways revealed by embedded correlated wavefunction theory. *ACS Nano* **13**, 9944 (2019).
197. Bao, J. L. & Carter, E. A. Rationalizing the hot-carrier-mediated reaction mechanisms and kinetics for ammonia decomposition on ruthenium-doped copper nanoparticles. *J. Am. Chem. Soc.* **141**, 13320 (2019).
198. Zhou, L. et al. Light-driven methane dry reforming with single atomic site antenna-reactor plasmonic photocatalysts. *Nat. Energy* **5**, 61 (2020).
199. Robatjazi, H. et al. Plasmon-driven carbon–fluorine (C(sp3)–F) bond activation with mechanistic insights into hot-carrier-mediated pathways. *Nat. Catal.* **3**, 564 (2020).
200. Zhou, L. et al. Hot carrier multiplication in plasmonic photocatalysis. *Proc. Natl Acad. Sci. USA* **118**, e2022109118 (2021).
201. Yuan, L. et al. Plasmonic photocatalysis with chemically and spatially specific antenna-dual reactor complexes. *ACS Nano* **16**, 17365 (2022).
202. Mennucci, B. & Corni, S. Multiscale modelling of photoinduced processes in composite systems. *Nat. Rev. Chem.* **3**, 315 (2019).
203. Morzan, U. N. et al. Spectroscopy in complex environments from qm-mm simulations. *Chem. Rev.* **118**, 4071 (2018).
204. Becca, J. C., Chen, X. & Jensen, L. A discrete interaction model/quantum mechanical method for simulating surface-enhanced raman spectroscopy in solution. *J. Chem. Phys.* **154**, 224705 (2021).
205. Romanelli, M., Dall'Osto, G. & Corni, S. Role of metal-nanostructure features on tip-enhanced photoluminescence of single molecules. *J. Chem. Phys.* **155**, 214304 (2021).
206. Urbieta, M. et al. Atomic-scale lightning rod effect in plasmonic picocavities: a classical view to a quantum effect. *ACS Nano* **12**, 585 (2018).
207. Yang, B. et al. Sub-nanometre resolution in single-molecule photoluminescence imaging. *Nat. Photon.* **14**, 693 (2020).
208. Russo, R., Fihey, A., Mennucci, B. & Jacquemin, D. Theoretical quantification of the modified photoactivity of photochromes grafted on metallic nanoparticles. *J. Phys. Chem. C* **120**, 21827 (2016).
209. Rinkevicius, Z. et al. Hybrid complex polarization propagator/molecular mechanics method for heterogeneous environments. *J. Chem. Theory Comput.* **12**, 2661 (2016).
210. Fihey, A., Maurel, F. & Perrier, A. Plasmon-excitation coupling for dithienylethene/gold nanoparticle hybrid systems: a theoretical study. *J. Phys. Chem. C* **119**, 9995 (2015).
211. Payton, J. L., Morton, S. M., Moore, J. E. & Jensen, L. A hybrid atomistic electrodynamics-quantum mechanical approach for simulating surface-enhanced raman scattering. *Acc. Chem. Res.* **47**, 88 (2014).
212. Morton, S. M. & Jensen, L. A discrete interaction model/quantum mechanical method for describing response properties of molecules adsorbed on metal nanoparticles. *J. Chem. Phys.* **133**, 074103 (2010).
213. Payton, J. L., Morton, S. M., Moore, J. E. & Jensen, L. A discrete interaction model/quantum mechanical method for simulating surface-enhanced raman spectroscopy. *J. Chem. Phys.* **136**, 214103 (2012).
214. Rinkevicius, Z., Li, X., Sandberg, J. A. R., Mikkelsen, K. V. & Ågren, H. A hybrid density functional theory/molecular mechanics approach for linear response properties in heterogeneous environments. *J. Chem. Theory Comput.* **10**, 989 (2014).
215. Corni, S. & Tomasi, J. Excitation energies of a molecule close to a metal surface. *J. Chem. Phys.* **117**, 7266 (2002).
216. Vukovic, S., Corni, S. & Mennucci, B. Fluorescence enhancement of chromophores close to metal nanoparticles. optimal setup revealed by the polarizable continuum model. *J. Phys. Chem. C* **113**, 121 (2009).
217. Masiello, D. J. & Schatz, G. C. Many-body theory of surface-enhanced raman scattering. *Phys. Rev. A* **78**, 042505 (2008).
218. Masiello, D. J. & Schatz, G. C. On the linear response and scattering of an interacting molecule-metal system. *J. Chem. Phys.* **132**, 064102 (2010).
219. Masiello, D. J. Multiscale theory and simulation of plasmon-enhanced molecular optical processes. *Int. J. Quant. Chem.* **114**, 1413 (2014).
220. Pipolo, S. & Corni, S. Real-time description of the electronic dynamics for a molecule close to a plasmonic nanoparticle. *J. Phys. Chem. C* **120**, 28774 (2016).
221. Coccia, E., Troiani, F. & Corni, S. Probing quantum coherence in ultrafast molecular processes: an ab initio approach to open quantum systems. *J. Chem. Phys.* **148**, 204112 (2018).
222. Dall'Osto, G. et al. Peeking into the femtosecond hot-carrier dynamics reveals unexpected mechanisms in plasmonic photocatalysis. *J. Am. Chem. Soc.* **146**, 2208 (2024).
223. Sakko, A., Rossi, T. P. & Nieminen, R. M. Dynamical coupling of plasmons and molecular excitations by hybrid quantum/classical calculations: time-domain approach. *J. Phys.: Condens. Matter* **26**, 315013 (2014).
224. Gao, Y. & Neuhauser, D. Communication: dynamical embedding: correct quantum response from coupling tddft for a small cluster with classical near-field electrodynamics for an extended region. *J. Chem. Phys.* **138**, 181105 (2013).
225. Caprasecca, S., Corni, S. & Mennucci, B. Shaping excitons in light-harvesting proteins through nanoplasmonics. *Chem. Sci.* **9**, 6219 (2018).
226. Caprasecca, S., Guido, C. A. & Mennucci, B. Control of coherences and optical responses of pigment-protein complexes by plasmonic nanoantennae. *J. Phys. Chem. Lett.* **7**, 2189 (2016).
227. Stefanucci, G. & van Leeuwen, R., *Nonequilibrium Many-Body Theory of Quantum Systems* (Cambridge University Press, 2013).
228. Caruso, F. & Zacharias, M. Quantum theory of light-driven coherent lattice dynamics. *Phys. Rev. B* **107**, 54102 (2023).

229. Fregoni, J., Granucci, G., Coccia, E., Persico, M. & Corni, S. Manipulating azobenzene photoisomerization through strong light–molecule coupling. *Nat. Commun.* **9**, 4688 (2018).
230. Gardner, J., Habershon, S. & Maurer, R. J. Assessing mixed quantum-classical molecular dynamics methods for nonadiabatic dynamics of molecules on metal surfaces. *J. Phys. Chem. C* **127**, 15257 (2023).
231. Albareda, G., Kelly, A. & Rubio, A. Nonadiabatic quantum dynamics without potential energy surfaces. *Phys. Rev. Mater.* **3**, 023803 (2019).
232. Mannouch, J. R. & Richardson, J. O. A mapping approach to surface hopping. *J. Chem. Phys.* **158**, 104111 (2023).
233. René Jestädt, M. J. T. O. A. R., Ruggenthaler, M. & Appel, H. Light-matter interactions within the ehrenfest-maxwell-pauli-kohn-sham framework: fundamentals, implementation, and nano-optical applications. *Adv. Phys.* **68**, 225 (2019).
234. Schäfer, C. & Johansson, G. Shortcut to self-consistent light-matter interaction and realistic spectra from first principles. *Phys. Rev. Lett.* **128**, 156402 (2022).
235. Sukharev, M. Efficient parallel strategy for molecular plasmonics - a numerical tool for integrating maxwell-schrödinger equations in three dimensions. *J. Comput. Phys.* **477**, 111920 (2023).
236. de Melo, P. M. M. C. & Marini, A. Unified theory of quantized electrons, phonons, and photons out of equilibrium: a simplified ab initio approach based on the generalized baym-kadanoff ansatz. *Phys. Rev. B* **93**, 155102 (2016).
237. Lacombe, L., Hoffmann, N. M. & Maitra, N. T. Exact potential energy surface for molecules in cavities. *Phys. Rev. Lett.* **123**, 083201 (2019).
238. Puértolas, B., Comesaña-Hermo, M., Besteiro, L. V., Vázquez-González, M. & Correa-Duarte, M. A. Challenges and opportunities for renewable ammonia production via plasmon-assisted photocatalysis. *Adv. Energy Mater.* **12**, 2103909 (2022).
239. Graziano, G. All-plasmonic water splitting. *Nat. Nanotechnol.* **16**, 1053 (2021).
240. Cortés, E. Catalysts light a path to sustainable chemistry. *Nature* **614**, 230 (2023).
241. Yuan, L., Bourgeois, B. B., Carlin, C. C., Da Jornada, F. H. & Dionne, J. A. Sustainable chemistry with plasmonic photocatalysts. *Nanophotonics* **12**, 2745–2762 (2023).
242. Blase, X., Duchemin, I. & Jacquemin, D. The Bethe-Salpeter equation in chemistry: relations with TD-DFT, applications and challenges. *Chem. Soc. Rev.* **47**, 1022 (2018).
243. Ezendam, S. et al. Hybrid plasmonic nanomaterials for hydrogen generation and carbon dioxide reduction. *ACS Energy Lett.* **7**, 778 (2022).
244. Collins, S. S. et al. Plasmon energy transfer in hybrid nanoantennas. *ACS Nano* **15**, 9522 (2021).
245. Lee, H. E. et al. Amino-acid- A nd peptide-directed synthesis of chiral plasmonic gold nanoparticles. *Nature* **556**, 360 (2018).
246. Lee, H. E. et al. Cysteine-encoded chirality evolution in plasmonic rhombic dodecahedral gold nanoparticles. *Nat. Commun.* **11**, 263 (2020).
247. Jiang, X. et al. Plasmonic active "hot spots"-confined photocatalytic CO2 reduction with high selectivity for CH4 production. *Adv. Mater.* **34**, 2109330 (2022).
248. Swearer, D. F. et al. Plasmonic photocatalysis of nitrous oxide into N2 and O2 using aluminum-iridium antenna-reactor nanoparticles. *ACS Nano* **13**, 8076 (2019).
249. Lyu, P. T. et al. Periodic distributions and ultrafast dynamics of hot electrons in plasmonic resonators. *Nano Lett.* **23**, 2262 (2023).
250. Kuttruff, J. et al. Sub-picosecond collapse of molecular polaritons to pure molecular transition in plasmonic photoswitch-nanoantennas. *Nat. Commun.* **14**, 3875 (2023).
251. Fregoni, J., Granucci, G., Persico, M. & Corni, S. Strong coupling with light enhances the photoisomerization quantum yield of azobenzene. *Chem.* **6**, 250 (2020).
252. Fregoni, J. et al. Strong coupling between localized surface plasmons and molecules by coupled cluster theory. *Nano Lett.* **21**, 6664 (2021).
253. Nan, L. et al. Investigating plasmonic catalysis kinetics on hot-spot engineered nanoantennae. *Nano Lett.* **23**, 2883 (2023).
254. Melendez, L. V., Van Embden, J., Connell, T. U., Duffy, N. W. & Gómez, D. E. Optimal geometry for plasmonic hot-carrier extraction in metal-semiconductor nanocrystals. *ACS Nano* **17**, 4659 (2023).
255. Zhang, C., Luo, Y., Maier, S. A. & Li, X. Recent progress and future opportunities for hot carrier photodetectors: from ultraviolet to infrared bands. *Laser Photon. Rev.* **16**, 2100714 (2022).
256. Fang, Y., Verre, R., Shao, L., Nordlander, P. & Käll, M. Hot electron generation and cathodoluminescence nanoscopy of chiral split ring resonators. *Nano Lett.* **16**, 5183 (2016).
257. Kang, B. et al. Local controllability of hot electron and thermal effects enabled by chiral plasmonic nanostructures. *Nanophotonics* **11**, 1195 (2022).
258. Wang, W. et al. Generation of hot electrons with chiral metamaterial perfect absorbers: giant optical chirality for polarization-sensitive photochemistry. *ACS Photon.* **6**, 3241 (2019).
259. Toffoli, D. et al. Circularly polarized plasmons in chiral gold nanowires via quantum-mechanical design. *J. Phys. Chem. Lett.* **12**, 5829 (2021).
260. Monti, M. et al. The conformational dynamics of the ligands determines the electronic circular dichroism of the chiral Au38(SC2h4Ph)24 cluster. *J. Phys. Chem. Lett.* **14**, 1941 (2023).
261. Monti, M. et al. What contributes to the measured chiral optical response of the glutathione-protected Au25 nanocluster? *ACS Nano* **17**, 11481 (2023).
262. Masson, J. F., Biggins, J. S. & Ringe, E. Machine learning for nanoplasmonics. *Nat. Nanotechnol.* **18**, 111 (2023).
263. Marinica, D., Kazansky, A., Nordlander, P., Aizpurua, J. & Borisov, A. G. Quantum plasmonics: nonlinear effects in the field enhancement of a plasmonic nanoparticle dimer. *Nano Lett.* **12**, 1333 (2012).
264. O'Keeffe, P. et al. Disentangling the temporal dynamics of nonthermal electrons in photoexcited gold nanostructures. *Laser Photon. Rev.* **15**, 2100017 (2021).
265. Mazzanti, A. et al. Light-heat conversion dynamics in highly diversified water-dispersed hydrophobic nanocrystal assemblies. *Proc. Natl Acad. Sci. USA* **116**, 8161 (2019).
266. João, S. M., Jin, H. & Lischner, J. C. Atomistic theory of hot-carrier relaxation in large plasmonic nanoparticles. *J. Phys. Chem. C* **127**, 23296 (2023).
267. Bonafé, F. P. et al. Plasmon-driven sub-picosecond breathing of metal nanoparticles. *Nanoscale* **9**, 12391 (2017).
268. Ranasingha, O. et al. Slow relaxation of surface plasmon excitations in Au55: the key to efficient plasmonic heating in Au/TiO2. *J. Phys. Chem. Lett.* **7**, 1563 (2016).
269. Wu, X. et al. Investigation of plasmon relaxation mechanisms using nonadiabatic molecular dynamics. *J. Chem. Phys.* **157**, 214201 (2022).
270. Clarivate. https://www.webofscience.com/wos/woscc/basic-search *Web Of Science* (2024)
271. Birkle, C., Pendlebury, D. A., Schnell, J. & Adams, J. Web of science as a data source for research on scientific and scholarly activity. *Quant. Sci. Stud.* **1**, 363 (2020).
272. Yan, L., Fu, Z. & Zhang, Z. *Plasmon-enhanced Light-matter Interactions* (eds Yu, P., Xu, H. & Wang, Z. M.) pp. 155–175 (Springer International Publishing, Cham, 2022).

Acknowledgements

M.V. acknowledges the University of Milan for funding his postdoctoral fellowships "La bellezza degli aggregati: da nano a astro particelle". M.V. also acknowledge support from the University of Milan through the APC initiative. Finally, M.V. thanks Prof. Francesca Baletto for her guidance and valuable suggestions. Certain data included herein are derived from Clarivate Web of Science.

Author contributions

M.V. designed the figures, collected and updated the literature; M.M. conceived the work and collected an initial literature core. Both authors summarized the literature and wrote the manuscript.

Competing interests

The authors declare no competing interests.

Additional information

Supplementary information The online version contains supplementary material available at https://doi.org/10.1038/s41524-024-01412-5.

Correspondence and requests for materials should be addressed to Mirko Vanzan or Margherita Marsili.